Article

Cell Reports

The Secreted Protein C1QL1 and Its Receptor BAI3 Control the Synaptic Connectivity of Excitatory Inputs Converging on Cerebellar Purkinje Cells

Graphical Abstract

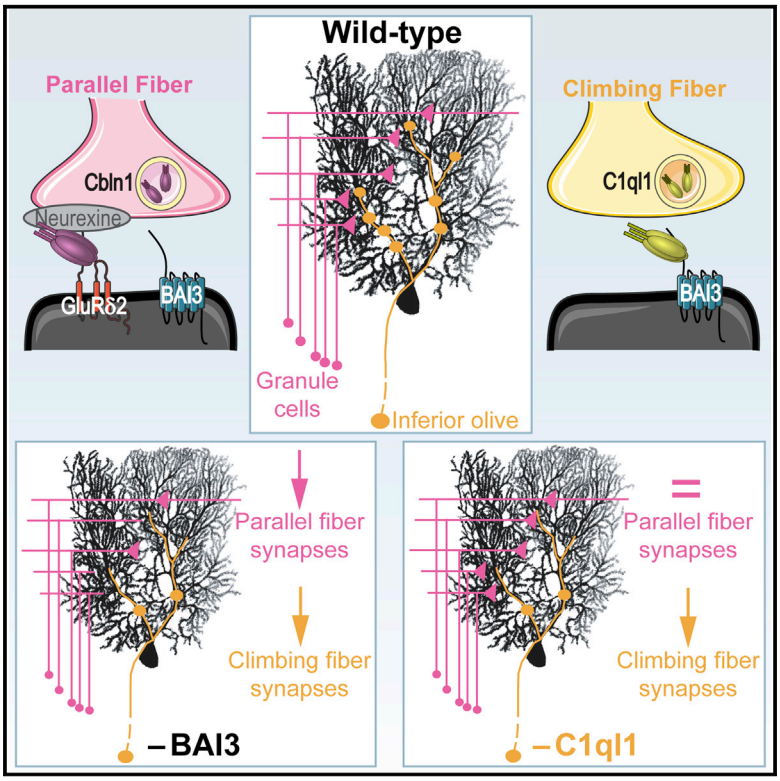

Authors

Séverine M. Sigoillot, Keerthana Iyer, ..., Philippe Isope, Fekrije Selimi

Correspondence

fekrije.selimi@college-de-france.fr

In Brief

Sigoillot et al. show that the adhesion-GPCR BAI3 and its ligand C1QL1 contribute to synapse specificity during development. The BAI3 receptor regulates synaptogenesis for both types of excitatory inputs on cerebellar Purkinje cells, whereas C1QL1 promotes proper synaptogenesis and innervation territory for only one type, the climbing fiber.

Highlights

- C1QL and BAI3 proteins are highly expressed during synaptogenesis
- BAI3 promotes spinogenesis and excitatory synaptogenesis in Purkinje cells
- C1QL1 controls climbing fiber synaptogenesis and territory on Purkinje cells
- C1QL1's modulation of Purkinje cell spinogenesis is BAI3 dependent

Sigoillot et al., 2015, Cell Reports *10*, 1–13
February 10, 2015 ©2015 The Authors
http://dx.doi.org/10.1016/j.celrep.2015.01.034

CellPress

Please cite this article in press as: Sigoillot et al., The Secreted Protein C1QL1 and Its Receptor BAI3 Control the Synaptic Connectivity of Excitatory Inputs Converging on Cerebellar Purkinje Cells, Cell Reports (2015), http://dx.doi.org/10.1016/j.celrep.2015.01.034

Cell Reports
Article

The Secreted Protein C1QL1 and Its Receptor BAI3 Control the Synaptic Connectivity of Excitatory Inputs Converging on Cerebellar Purkinje Cells

Séverine M. Sigoillot,[1] Keerthana Iyer,[1] Francesca Binda,[2] Inés González-Calvo,[1,2] Maëva Talleur,[1] Guilan Vodjdani,[3] Philippe Isope,[2] and Fekrije Selimi[1,*]
[1]Center for Interdisciplinary Research in Biology (CIRB), Collège de France; CNRS UMR 7241; and INSERM U1050, Paris 75005, France
[2]Institut des Neurosciences Cellulaires et Intégratives, CNRS UPR 3212, Université de Strasbourg, Strasbourg 67084, France
[3]Neuroprotection du Cerveau en Développement (PROTECT), INSERM, UMR1141, Université Paris-Diderot, Sorbonne Paris-Cité, Paris 75019, France
*Correspondence: fekrije.selimi@college-de-france.fr
http://dx.doi.org/10.1016/j.celrep.2015.01.034

SUMMARY

Precise patterns of connectivity are established by different types of afferents on a given target neuron, leading to well-defined and non-overlapping synaptic territories. What regulates the specific characteristics of each type of synapse, in terms of number, morphology, and subcellular localization, remains to be understood. Here, we show that the signaling pathway formed by the secreted complement C1Q-related protein C1QL1 and its receptor, the adhesion-GPCR brain angiogenesis inhibitor 3 (BAI3), controls the stereotyped pattern of connectivity established by excitatory afferents on cerebellar Purkinje cells. The BAI3 receptor modulates synaptogenesis of both parallel fiber and climbing fiber afferents. The restricted and timely expression of its ligand C1QL1 in inferior olivary neurons ensures the establishment of the proper synaptic territory for climbing fibers. Given the broad expression of C1QL and BAI proteins in the developing mouse brain, our study reveals a general mechanism contributing to the formation of a functional brain.

INTRODUCTION

In the nervous system, each type of neuron is connected to its afferents in a stereotyped pattern that is essential for the proper integration of information and brain function. A neuron can receive several convergent inputs from different neuronal populations with specific characteristics. The number and the subcellular localization of synapses from each afferent on a target neuron are determined by a complex developmental process that involves recognition, repulsion, elimination of supernumerary synapses, and/or guidance posts (Sanes and Yamagata, 2009; Shen and Scheiffele, 2010). How these precise patterns of connectivity are established is likely to vary depending on the neuronal population and remains a poorly understood question.

Several classes of adhesion proteins, such as cadherins, immunoglobulin-superfamily (IgSF) proteins, neuroligins, and leucine-rich repeats transmembrane (LRRTM) proteins, have been involved in synapse formation, maturation, and function (Shen and Scheiffele, 2010). In addition, secreted proteins, such as WNTs (Salinas, 2012), pentraxins (Sanes and Yamagata, 2009; Shen and Scheiffele, 2010; Sia et al., 2007), or CBLNs (Yuzaki, 2011), can regulate synapse formation and function, both in an anterograde and retrograde manner. This molecular diversity and functional redundancy is in agreement with the idea that a specific set of molecular pathways defines each combination of afferent-target neuron in the vertebrate brain (O'Rourke et al., 2012; Sperry, 1963).

Molecular signaling pathways regulate different aspects of synapse specificity. Adhesion proteins, such as IgSF members sidekicks in the retina (Yamagata and Sanes, 2008), can have an instructive role for the choice of the synaptic partners and also determine the balance of inhibitory versus excitatory connectivity, as illustrated by the studies of neuroligins (Südhof, 2008). Further specificity resides in the definition of non-overlapping territories for inhibitory and excitatory synapses on a given neuron. For example, Purkinje cells receive two types of excitatory inputs (parallel fibers from granule cells and climbing fibers from inferior olivary neurons) and two types of inhibitory inputs (from basket cells and stellate cells), which form synapses on separate and non-overlapping territories. Adhesion proteins from the L1 Ig subfamily have been shown to control the specific subcellular localization of each inhibitory synapse (Ango et al., 2004, 2008). A very recent study of Ce-Punctin, an ADAMTS-like secreted protein, in the invertebrate nervous system has shown that specific isoforms are secreted by cholinergic and inhibitory inputs and control the proper localization of corresponding synapses at the neuromuscular junction (Pinan-Lucarré et al., 2014). Thus, in addition to adhesion proteins, the specific secretion of some factors could play an important role in defining synapse specificity.

In the vertebrate brain, the complement C1Q-related proteins comprise several subfamilies: proteins related to the innate

Please cite this article in press as: Sigoillot et al., The Secreted Protein C1QL1 and Its Receptor BAI3 Control the Synaptic Connectivity of Excitatory Inputs Converging on Cerebellar Purkinje Cells, Cell Reports (2015), http://dx.doi.org/10.1016/j.celrep.2015.01.034

immunity factor C1Q, some of which have been involved in synapse elimination (Stevens et al., 2007), CBLNs known for promoting synapse formation (Yuzaki, 2011), and the C1Q-like (C1QL) subfamily. Proteins of this last subclass were recently shown to be high-affinity binding partners of the adhesion G-protein-coupled receptor (GPCR) brain angiogenesis inhibitor 3 (BAI3) and to promote synapse elimination in cultured hippocampal neurons (Bolliger et al., 2011). Our understanding of the function of brain angiogenesis inhibitor receptors in synaptogenesis is limited. The BAI3 receptor has been identified in biochemical preparations of synapses both in the forebrain (Collins et al., 2006) and in the cerebellum (Selimi et al., 2009), and recently, BAI1 was shown to promote spinogenesis and synaptogenesis through its activation of RAC1 in cultured hippocampal neurons (Duman et al., 2013). Interestingly, the BAI proteins have been associated with several psychiatric symptoms by human genetic (DeRosse et al., 2008; Liao et al., 2012) or functional studies (Okajima et al., 2011) and could thus directly be involved in the synaptic defects found in these disorders. In the present study, we explored the role of the C1QL/BAI3 signaling pathway in the establishment of specific neuronal networks using a combination of expression and functional studies in the developing mouse brain. Our results show that the temporally and spatially controlled expression of C1QL1 and the presence of its receptor, the adhesion-GPCR BAI3, in target neurons are key determinants of excitatory synaptogenesis and innervation territories in the vertebrate brain.

RESULTS

The Spatiotemporal Expression Pattern of the C1QL Ligands and Their BAI3 Receptor Is in Agreement with a Role in Neuronal Circuit Formation

The adhesion-GPCR BAI3 has been found at excitatory synapses by biochemical purifications (Collins et al., 2006; Selimi et al., 2009). In transfected hippocampal neurons, BAI3 is highly enriched in spines and is found to colocalize with and surround clusters of the postsynaptic marker PSD95 using immunocytochemistry (Figure S1). Together with the fact that BAI receptors can modulate RAC1 activity, a major regulator of the actin cytoskeleton, in neurons (Duman et al., 2013; Lanoue et al., 2013), these data suggest a function for the BAI3 receptor in the control of synaptogenesis. To play this role, the timing and pattern of BAI3 expression should be in agreement with the timing of synaptogenesis. In situ hybridization experiments showed that *Bai3* mRNAs are highly expressed in the mouse brain during the first 2 postnatal weeks, in regions of intense synaptogenesis such as the hippocampus, cortex, and cerebellum (Figure 1A). In the cerebral cortex, a gradient of *Bai3* expression is observed with the highest level at postnatal day 0 (P0) in the deep layers and at P7 in the most superficial layer, reminiscent of the inside-out development of this structure. At these stages, *Bai3* is also expressed in the brainstem, in particular in the basilar pontine nucleus and the inferior olive, and in the cerebellum (Figure 1A). In the adult mouse brain, *Bai3* expression decreases in many regions, such as in the brainstem (assessed by qRT-PCR; Figure 1B) and becomes restricted to a few neuronal populations, such as cerebellar Purkinje cells, pyramidal cells in the hippocampus, and neurons in the cerebral cortex (Figures 1A and S2).

Secreted C1QL proteins of the C1Q complement family can bind the BAI3 receptor with high affinity (Bolliger et al., 2011) and could thus regulate its synaptic function. In situ hybridization experiments (Figure 1), in accordance with previously published data (Iijima et al., 2010), show that *C1ql* mRNAs, in particular *C1ql1* and *C1ql3*, are highly expressed during the first 2 postnatal weeks in various neuronal populations. *C1ql3* mRNA is found in the cortex, lateral amygdala, dentate gyrus, and deep cerebellar nuclei. *C1ql1* is very highly expressed in the inferior olive at all stages, including in the adult. It is also found at P0 and P7 in neurons of the hippocampus, cerebral cortex, and in few other neurons of the brainstem. By qRT-PCR, we also detected *C1ql1* expression in the cerebellum, with a peak at P7 at a level that is 5-fold less than in the brainstem. This transient cerebellar expression is in agreement with previous in situ hybridization data that showed expression of *C1ql1* in the external granular layer of the developing cerebellum (Iijima et al., 2010).

This expression analysis shows that C1QL proteins are produced in neurons that are well-described afferents of neurons expressing BAI3, such as inferior olivary neurons that connect Purkinje cells (PCs). It also indicates that different C1QL/BAI3 complexes could control synaptogenesis in various regions of the brain. The C1QL3/BAI3 complex is prominent in the cortex and hippocampus, whereas the C1QL1/BAI3 complex might be particularly important for excitatory synaptogenesis on cerebellar PCs. Indeed, the expression pattern of the C1QL1/BAI3 couple correlates with the developmental time course of excitatory synaptogenesis in PCs: these neurons receive their first functional synapses from the climbing fibers, the axons of the inferior olivary neurons, on their somata around P3, at a time when *C1ql1* mRNA expression starts to increase sharply (Figures 1A and 1B), and when *Bai3* mRNA is already found in PCs (Figures 1 and S2). PCs are subject to an intense period of synaptogenesis with their second excitatory inputs, the parallel fibers, starting at P14, when *Bai3* expression in the cerebellum reaches its maximum (Figure 1B). Given the well-described timing and specificity of PC excitatory connectivity, we focused our studies on the olivocerebellar network to identify the function of the C1QL/BAI3 complexes during the formation of neuronal circuits.

The Adhesion-GPCR BAI3 Promotes the Development of Excitatory Synaptic Connectivity on Cerebellar PCs

Inferior olivary neurons send their axons to the cerebellum, where they start forming functional synapses on somata of PCs at around P3. These projections mature into climbing fibers (CFs) while PCs develop their dendritic arbor during the second postnatal week. Starting at P9, a single CF translocates and forms a few hundred synapses on thorny spines of PC proximal dendrites (Hashimoto et al., 2009). Each PC also receives information from up to 175,000 parallel fibers (PFs) through synapses formed on distal dendritic spines, in particular during the second and third postnatal weeks (Sotelo, 1990). To test the role of the BAI3 receptor during the development of the olivocerebellar network, we developed an RNAi approach: two different short hairpin RNAs targeting different regions of the *Bai3* mRNA

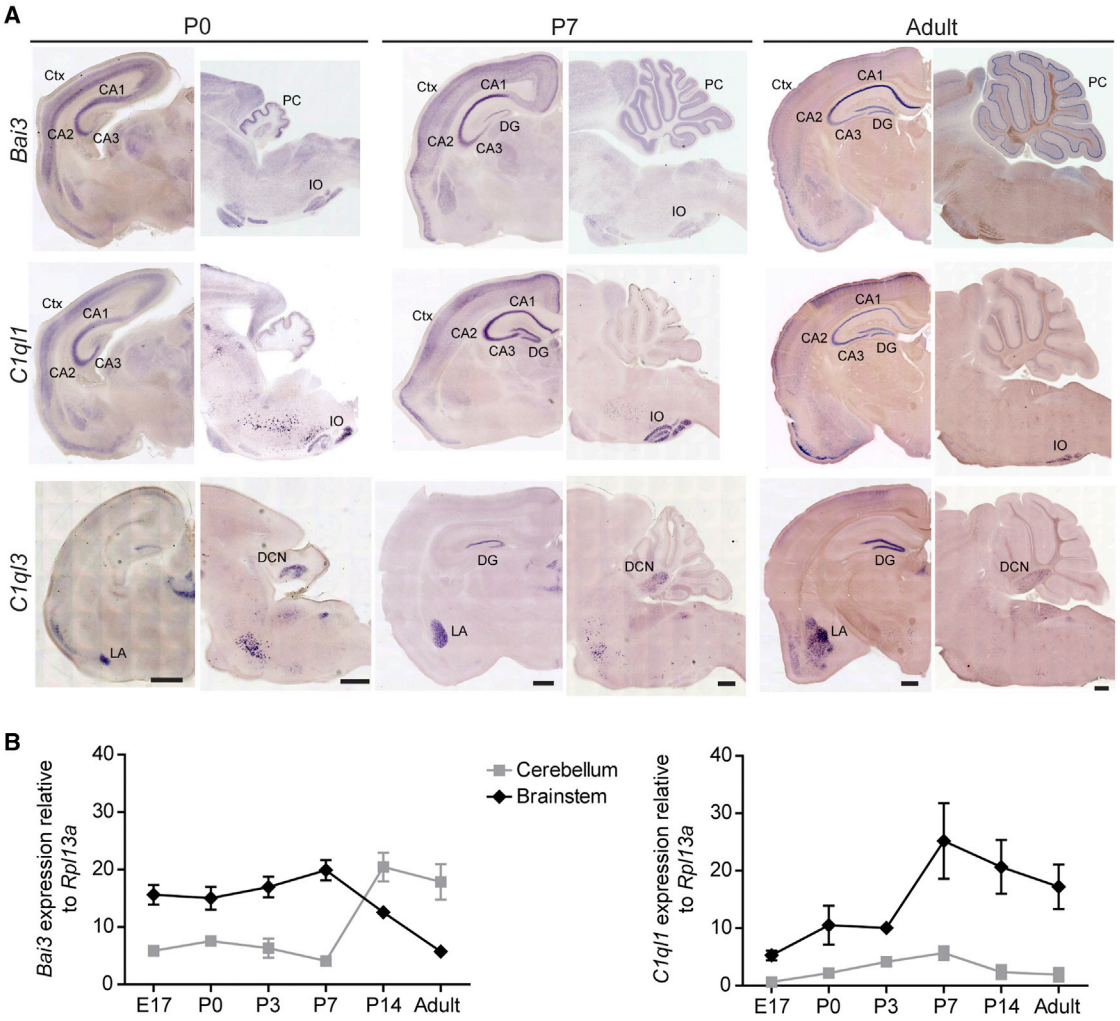

Figure 1. Developmentally Regulated Expression of the *Bai3* and *C1ql* Genes in the Mouse Brain

(A) In situ hybridization experiments were performed using probes specific for *Bai3*, *C1ql1*, and *C1ql3* on coronal (left) and sagittal (right) sections of mouse brain taken at postnatal day 0 (P0), P7, and adult. Ctx, cortex; DCN, deep cerebellar nuclei; DG, dentate gyrus; Hp, hippocampus; IO, inferior olive; LA, lateral amygdala; PC, Purkinje cell. The scale bars represent 500 μm; each scale bar applies to the whole column.

(B) Expression of *Bai3* and *C1ql1* was assessed at different stages of mouse brain development with qRT-PCR on mRNA extracts from brainstem and cerebellum (E17, embryonic day 17; P0–P14, postnatal day 0 to 14). Expression levels are normalized to the *Rpl13a* gene. n = 3 samples per stage. Data are presented as mean ± SEM.

See also Figure S2.

(shBAI3) were designed and selected after testing their efficiency in transfected HEK293 cells (data not shown). A lentiviral vector was then used to drive their expression in neurons both in vivo and in vitro, together with the expression of enhanced GFP (eGFP; under the control of the ubiquitous PGK1 promoter). In mixed cerebellar cultures transduced at 4 days in vitro (DIV4), both shRNAs led to about 50% knockdown of *Bai3* by DIV7 and did not affect the expression level of another PC-expressed gene, *Pcp2*, confirming their specificity (Figure S3A). Knockdown of *Bai3* was still present after 10 days in culture (Figure S3A). Morphological analysis in mixed cerebellar cultures confirmed that both shRNAs against *Bai3* induced the same phenotype (cf. below). Because one of the shRNA constructs was more efficient (similar levels of knockdown with half the amount of lentiviral particles), it was chosen for in vivo experiments.

Recombinant lentiviral particles driving either shBAI3 or a control non-targeting shRNA (shCTL) were injected in the molecular layer of the cerebellum of mouse pups at P7, when the most intense period of PF synaptogenesis starts and just before the translocation of the strongest CF (Hashimoto et al., 2009). *Bai3* knockdown induced visible deficits in the connectivity between CFs and their target PCs visualized at P21 using an antibody against VGLUT2, a specific marker of CF presynaptic boutons in the molecular layer (Figure 2). The extension of the CF synaptic territory on arbors of PCs expressing shBAI3 was reduced by about 35% when compared to shCTL-expressing PCs (Figures 2A and 2C). This effect is

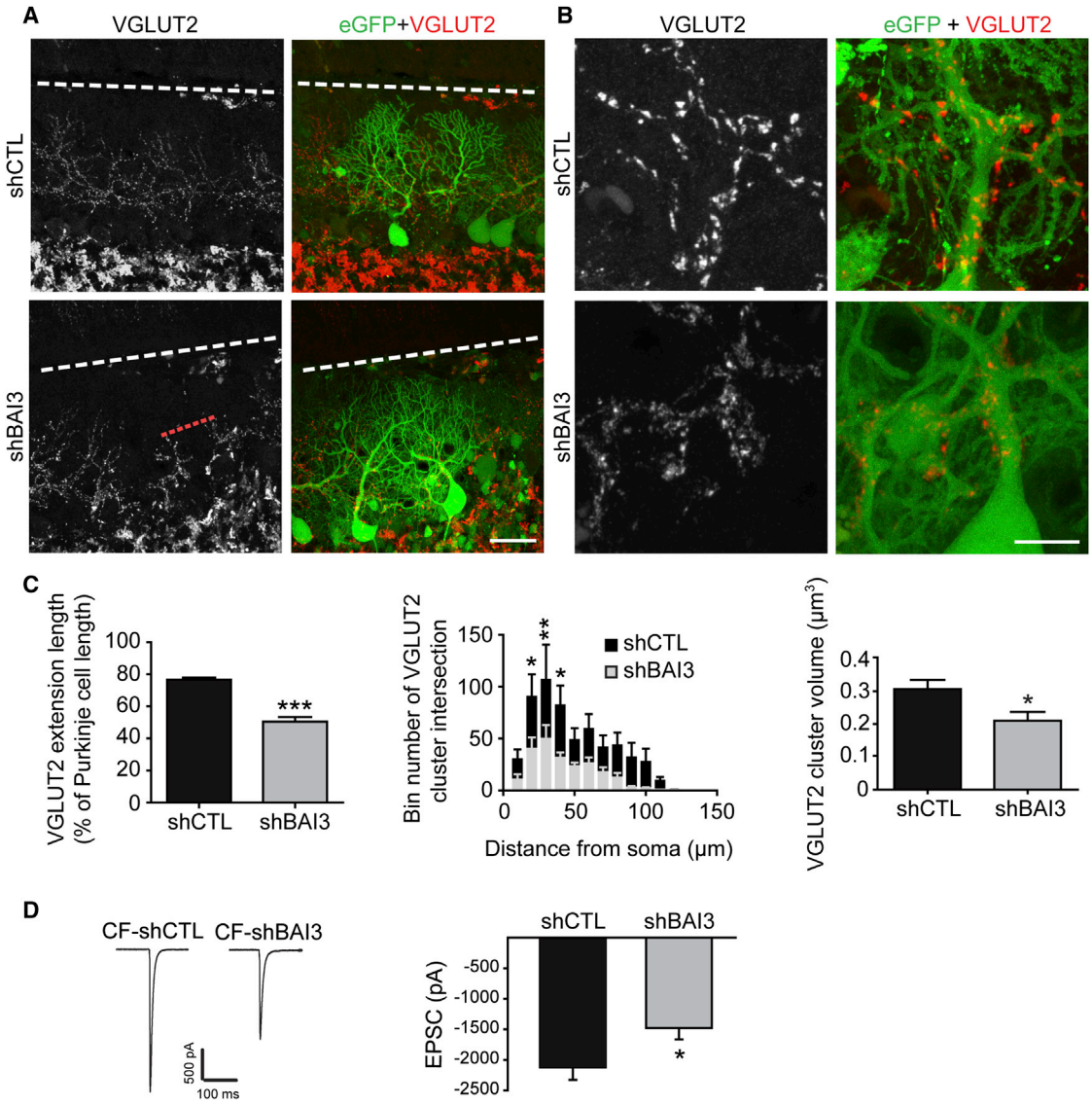

Figure 2. The Adhesion-GPCR BAI3 Promotes Synaptogenesis and the Innervation Territory of CFs on PCs

(A and B) Defects in CF synapses were assessed at P21 after stereotaxic injections at P7 of recombinant lentiviral particles driving expression of shRNA against *Bai3* (shBAI3) or control shRNA (shCTL). Immunostaining for vesicular glutamate transporter 2 (VGLUT2) was used to label specifically CF synapses on transduced PCs (eGFP positives). (A) Representative images of VGLUT2 extension. Pial surface: white dashed line. The scale bar represents 40 μm. (B) Representative images of VGLUT2 cluster morphology. The scale bar represents 10 μm.

(C) The extension of VGLUT2 clusters relative to PC height, their mean number, and volume were quantified using Image J. n ≥ 22 cells, n = 3 animals per condition. Data are presented as mean ± SEM; unpaired Student's t test or two-way ANOVA followed by Bonferroni post hoc test; *p < 0.05; **p < 0.01; ***p < 0.001.

(D) Electrophysiological recordings of P18–P23 PCs transduced with recombinant lentiviral particles driving expression of either shBAI3 or shCTL. CF-mediated whole-cell currents are shown in the left panel. Averages of five stimuli for two representative cells are shown. Traces were recorded at −10 mV following CF stimulation. Total CF-mediated EPSCs were quantified and plotted in the bar graph shown in the right panel. Bars represent mean ± SEM. Unpaired Student's t test; *p < 0.05.

See also Figures S3A and S4A.

cell-autonomous because it is not observed in non-eGFP PCs in the transduced region (Figure S4A). Quantification of synaptic puncta revealed a reduction in number (507.75 ± 109.94 versus 217.10 ± 37.21; *p ≤ 0.05, Student's unpaired t test) and volume (about 30%) of VGLUT2 clusters on shBAI3-PCs when compared to shCTL-PCs (Figure 2). These morphological changes were accompanied by a deficiency in CF transmission, as shown by the reduced whole-cell currents elicited by CF stimulation in PCs recorded in acute cerebellar slices from P18 to P23 mice (Figure 2D; shCTL = −2,122.54 ± 204.77 pA, n = 5 cells; shBAI3 = −1,478.6 ± 186.24 pA, n = 8 cells; Student's t test; *p < 0.05).

A reduced spine density was also evident at P21 in distal dendrites of shBAI3-PCs (Figure 3A), suggesting a potential defect in PF connectivity. To confirm this, we recorded PF-EPSCs of PCs and input-output relationships were examined. Their amplitudes gradually increased with PF stimulus intensity but reached a plateau for much smaller values of stimulation in BAI3-deficient PCs than in control PCs (Figure 3B). The high density of PF synapses in the cerebellar molecular layer impedes precise morphological quantifications of synaptic defects in transduced PCs in vivo. We thus turned to mixed cerebellar cultures that recapitulate PF synaptogenesis with similar characteristics as in vivo because, in this system, PCs develop highly branched dendrites studded with numerous spines on which granule cells form synapses. The effect of *Bai3* knockdown on PF/PC spinogenesis and synaptogenesis was assessed at DIV14, 10 days post-transduction, by co-immunolabeling followed by high-resolution confocal imaging and quantitative analysis. An antibody against the soluble calcium-binding protein CaBP allowed us to label PC dendrites and spines, and an antibody against the vesicular transporter VGLUT1 was used to label specifically the PF presynaptic boutons (Figure 3C). A reduced spine density and a decreased mean spine head diameter was measured on 3D-reconstructed dendrites after transduction of PCs with either of the two shRNAs targeting *Bai3* (32% and 22% for shRNA no. 1 and shRNA no. 2, respectively, when compared to shCTL; cf. Figures 3D and S5). A significant reduction in the density of PF contacts was also revealed in shBAI3-PCs compared to controls, at a level similar to the one observed for spine density (24% and 22% for shRNA no. 1 and shRNA no. 2, respectively; cf. Figures 3E and S5C). Both shRNAs against *Bai3* induced similar defects. These reductions in spine and synapse density were not observed in non-transduced (non-eGFP) PCs in transduced mixed cultures, showing that the effect of *Bai3* knockdown was cell-autonomous (Figures S4B and S4C). These results show that the adhesion-GPCR BAI3 regulates PF connectivity on PCs by controlling spinogenesis and synaptogenesis.

Thus, the adhesion-GPCR BAI3 is a general promoter of excitatory synaptogenesis during development of the olivocerebellar circuit, given that it controls the connectivity of both PF and CF excitatory inputs on cerebellar PCs.

The Ligand C1QL1 Is Indispensable for CF/PC Synaptogenesis

In the developing olivocerebellar circuit, *C1ql1* is expressed at high levels by inferior olivary neurons. The deficits in CF/PC synaptogenesis induced by knockdown of the adhesion-GPCR BAI3 suggested that the secretion of its ligand C1QL1 by CFs could also regulate this process. An RNAi approach was developed to target *C1ql1* by designing and selecting a shRNA efficient for *C1ql1* knockdown (shC1QL1) in transfected HEK293 cells (data not shown). To enable transduction of neurons in vitro and in vivo, this shRNA was then integrated in a lentiviral vector co-expressing eGFP under the ubiquitous PGK1 promoter. qRT-PCR analysis showed that a 90% reduction in *C1ql1* mRNA expression was induced by DIV7, 3 days post-transduction, an effect that was maintained at DIV14 (Figure S3B). *C1ql1* expression levels could be entirely restored by co-transduction with lentiviral particles driving the expression of a resistant *C1ql1* cDNA construct under the PGK1 promoter, but not by a wild-type *C1ql1* construct (Figure S3B).

The morphology and function of CF/PC synapses were assessed after injection of lentiviral particles driving shC1QL1 in the inferior olive of P4 neonates (Figure S6). This stage corresponds to the beginning of CF synaptogenesis on PC somata and precedes their translocation on PC dendrites (Figure S6). Compared to control shCTL-CFs that extended to 61% of the PC dendritic height by P14, there was a small but significant reduction in the extension of shC1QL1-CFs to about 56% (Figures 4A and 4B). There was little difference in the proportion of translocating CFs at P9 (11/35 for shCTL, 8/31 for shC1QL1, and 14/46 for shC1QL1+C1QL1 Rescue; Figure S6C). These results suggest that *C1ql1* knockdown in inferior olivary neurons has only a small effect on the ability of CFs to translocate. In contrast, the extension of the synaptic territory of shC1QL1-CFs, as assessed by anti-VGLUT2 immunolabeling, was decreased by half compared to control shCTL-CFs (30% and 60% of PC dendritic height, respectively; Figure 4). The mean number of VGLUT2-positive clusters per transduced CF was also reduced by 50% by *C1ql1* knockdown (Figure 4). Co-transduction with lentiviral particles driving the expression of the resistant *C1ql1* construct could partially rescue these phenotypes, showing that they were dependent on *C1ql1* expression (Figure 4). To confirm these synaptic phenotypes at the electrophysiology level, CF-EPSCs were recorded in PCs in acute slices from animals injected with shC1QL1 and shCTL lentiviral particles. Recordings were performed in lobule II, a region targeted by transduced CFs. A 49% decrease in CF transmission was observed in PCs from animals injected with shC1QL1 particles when compared to PCs from animals injected with shCTL particles (Figure 4C; shCTL = $-1{,}771.27 \pm 220.87$ pA, n = 8 cells; shC1QL1 = -907.59 ± 131.67 pA, n = 8 cells; Mann Whitney *U* test; $^*p < 0.05$). All together, these results show that *C1ql1* expression by CFs is indispensable for their normal connectivity on PCs.

Restriction of *C1ql1* Expression to CFs in the Cerebellum Is Necessary for Their Proper Innervation of the Target PC

The translocation of the "winner" CF on PC proximal dendrites starts at around P9 and continues until about P21, when the CF acquires its final synaptic territory (Figure 2; Hashimoto et al., 2009). At P7, just before CF translocation, the expression of *C1ql1* decreases in the cerebellum whereas it starts to increase in the brainstem to reach a plateau by P14 (Figure 1). To assess whether the specific expression pattern of *C1ql1* contributes to the acquisition of the final innervation territory of CFs on PCs, we misexpressed *C1ql1* in the cerebellum, by injecting lentiviral particles driving expression of a *C1ql1* cDNA (under the control of the PGK1 promoter) in the molecular layer at P7 (Figure 5). The synaptic territory of CFs on PC dendrites was significantly reduced at P14 by *C1ql1* misexpression when compared to eGFP controls (VGLUT2 puncta extending to 45% and 60% of PC height, respectively). Thus, the restricted and specific expression of *C1ql1* by inferior olivary neurons that is progressively established during development is

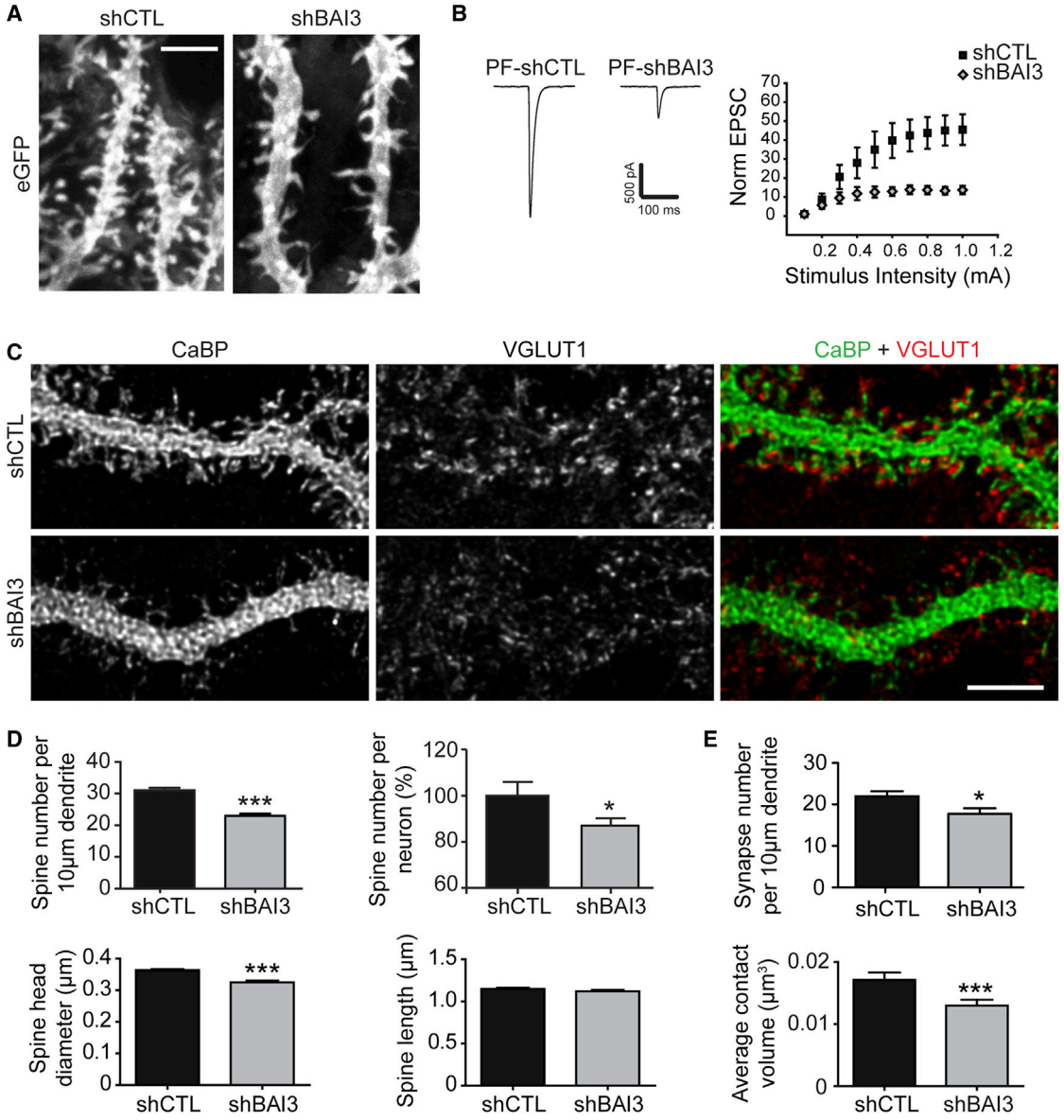

Figure 3. The Adhesion-GPCR BAI3 Promotes Spinogenesis and PF Synaptogenesis in PCs

(A) Reduced spine density in distal dendrites of PCs after in vivo knockdown of *Bai3* using stereotaxic injections of lentiviral particles in the vermis of P7 mice. Effects of shBAI3 or shCTL expression were visualized at P21 on transduced PCs (eGFP positives). The scale bar represents 5 µm.

(B) PF-ESPCs recorded in PCs (P18–P23) after stereotaxic injections of lentiviral particles at P7. Averaged traces recorded at maximum stimulus intensity are shown for one representative cell per condition (control: PF-shCTL, left; BAI3 knockdown: PF-shBAI3, right). Input/output curves obtained for both conditions are significantly different (right panel: Kolmogorov-Smirnov test; $p < 0.001$). Data are normalized to the mean value of responses elicited by the minimum stimulus intensity (-29.63 ± 9.92 pA for shCTL and -32.54 ± 10.57 pA for shBAI3) and are plotted as mean ± SEM against stimulus intensity (shCTL black square, n = 9, and shBAI3 gray diamond, n = 10).

(C) Cerebellar mixed cultures were transduced at DIV4 with recombinant lentiviral particles driving expression of eGFP together with shBAI3 or control shCTL. Dendritic spines and PF synapses in transduced PCs (eGFP positives) were imaged at DIV14 after immunostaining for calbindin (CaBP) and VGLUT1. The scale bar represents 5 µm.

(D) Quantitative assessment of the number and morphology of PC spines was performed using the NeuronStudio software. $n \geq 31$ cells per condition, three independent experiments (data are presented as mean ± SEM; unpaired Student's t test; *$p < 0.05$; ***$p < 0.001$).

(E) Quantitative assessment of the number and size of VGLUT1 synaptic contacts in DIV14 PCs was performed using ImageJ. $n \geq 30$ cells per condition, three independent experiments (data are presented as mean ± SEM; unpaired Student's t test and Mann-Whitney *U* test, respectively; *$p < 0.05$; ***$p < 0.001$).

See also Figures S3A, S4, and S5.

necessary for the development of the proper synaptic territory of the "winner" CF on the PC dendritic arbor.

The Ligand C1QL1 Promotes PC Spinogenesis in a BAI3-Dependent Manner

The deficits in PF spinogenesis and synaptogenesis induced by knockdown of the adhesion-GPCR BAI3 cannot be explained by its role in controlling CF/PC synaptogenesis. Because BAI3 has been identified at the PF/PC synapses (Selimi et al., 2009) and *C1ql1* is transiently expressed in the cerebellum (Figure 1B; Iijima et al., 2010), the C1QL1/BAI3 signaling pathway could directly regulate PC spinogenesis and PF synaptogenesis. We tested this hypothesis in cerebellar mixed cultures because the expression pattern of *C1ql1* in this system is similar to the pattern observed in vivo, with a peak at DIV7 (Figure S7). As for its receptor BAI3, the effects of *C1ql1* knockdown were assessed at DIV14, 10 days post-transduction, using CaBP and VGLUT1 immunostaining, high-resolution confocal imaging, and quantitative analysis. Our results show a 47% reduction in PC spine density, a small but significant increase in spine head diameter, but no effect on the mean spine length in shC1QL1-treated cultures compared to shCTL-treated ones (Figure 6). No change in the density of VGLUT1 contacts on PC spines was detected, suggesting that the proportion of PFs able to synapse on the available spines remains stable and that the reduction in spine density is overcome by an increase in the contact ratio between PFs and PCs in our culture system. All these effects were rescued by the concomitant expression of the resistant *C1ql1* cDNA construct, but not by a wild-type *C1ql1* cDNA driven by the same PGK1 promoter (Figure 6). Thus, C1QL1 secretion in the cerebellum modulates spine production in PCs, thereby regulating the amount of postsynaptic sites available for innervation by PFs.

C1QL proteins bind the BAI3 receptor with high affinity (Bolliger et al., 2011), suggesting that C1QL1 could regulate spinogenesis in PCs through the adhesion-GPCR BAI3. In this case, the simultaneous knockdown of both proteins should not induce an additive phenotype. Knockdown of both *Bai3* and *C1ql1*, by co-transduction of cerebellar cultures with a mixture of lentiviral particles, led to a 30% reduction in spine density, similar to the one observed for knockdown of *Bai3* only (Figure 7). Co-transduction of the control shCTL together with either shBAI3 or shC1QL1 induced the same level of spine reduction compared to shBAI3 or shC1QL1 alone (about 30% and 50%, respectively; Figures 3, 6, and 7), showing that there was no non-specific effect of co-transduction itself on spine density. A non-specific effect of shC1QL1 and shCTL co-expression prevented the interpretation of the data on spine morphology (Figure 7B). The level of reduction in spine density after double knockdown corresponds to the one detected for *Bai3* knockdown alone and is smaller than for *C1ql1* knockdown alone. Thus, whereas C1QL1 and BAI3 do not control spine density independently, their regulation of this process is complex.

DISCUSSION

Each neuron receives synapses from multiple types of afferents with specific morphological, quantitative, and physiological characteristics. These patterns are stereotyped for each type of neuronal population and are key to the proper integration of signals during brain function. Here, we show that the signaling pathway formed by the secreted protein C1QL1 and the adhesion-GPCR BAI3 regulates the development of proper excitatory connectivity on cerebellar PCs. First, the BAI3 receptor promotes both PF and CF connectivity on PCs and is thus a general regulator of excitatory synaptogenesis. Second, the C1QL1 protein is indispensable for proper CF/PC synaptogenesis and the development of the proper synaptic territory, but not for CF translocation. C1QL1 also modulates the production of the final number of distal dendritic spines by PCs, thereby regulating the number of available contact sites for PFs. Given the broad expression of the C1QL/BAI3 pathway in the developing brain, our study informs about a general mechanism used for the control of brain connectivity.

Most excitatory synapses are made on dendritic spines. In the cerebellum, studies of mouse mutants such as *weaver* and *reeler* indicate that PCs can generate spines through an intrinsic program (Sotelo, 1990). Whereas models involving the incoming axons in the process of spine induction have been put forward in other neuronal types such as cortical or hippocampal pyramidal cells, current data do not exclude an intrinsic program for spinogenesis in these neurons (Salinas, 2012; Yuste and Bonhoeffer, 2004). In all cases, the regulation of the actin cytoskeleton, in particular through modulation of RhoGTPases such as RAC1, is essential for the proper morphology and maturation of dendritic spines and associated synapses (Luo, 2002). The BAI receptors can regulate RAC1 activity both in neurons (Duman et al., 2013; Lanoue et al., 2013) and other cell types (Park et al., 2007). Our results show that, as BAI1 in cultured hippocampal neurons (Duman et al., 2013), the adhesion-GPCR BAI3 regulates spinogenesis in distal dendrites of PCs in vivo. PCs produce two types of spines: a small number of thorny spines on the proximal dendrites that are contacted by CFs and very dense spines on the distal dendrites that are contacted by PFs. In the adult cerebellum, PCs generate spines of the distal type in their proximal dendrites if the CF is removed through lesions or activity blockade (Rossi and Strata, 1995), showing an intrinsic ability to produce spines of this type. The adhesion-GPCR BAI3 could be part of this intrinsic program because its expression is maintained at high levels in adult PCs, contrary to many other neurons. Transient expression of *C1ql1* in the external granular layer (Figure 1; Iijima et al., 2010), by a yet-to-be defined cell type, during PC growth can modulate to a certain extent the number of spines produced in PCs, suggesting a local extrinsic regulation of the number of available contact sites for PFs.

Various classes of membrane adhesion proteins regulate the proper formation of mature excitatory synapses, including cadherins, neuroligins, and SynCAM (Shen and Scheiffele, 2010). Besides the well-described role of neurotrophins, increasing evidence also shows a role for other classes of secreted proteins, such as WNTs (Salinas, 2012) or complement C1Q-related proteins (Yuzaki, 2011). The complement C1Q-related family is composed of three different subfamilies: the classical C1Q-related; the cerebellins (CBLN); and the little-studied C1QL proteins. The classic C1Q complement protein promotes synapse

Please cite this article in press as: Sigoillot et al., The Secreted Protein C1QL1 and Its Receptor BAI3 Control the Synaptic Connectivity of Excitatory Inputs Converging on Cerebellar Purkinje Cells, Cell Reports (2015), http://dx.doi.org/10.1016/j.celrep.2015.01.034

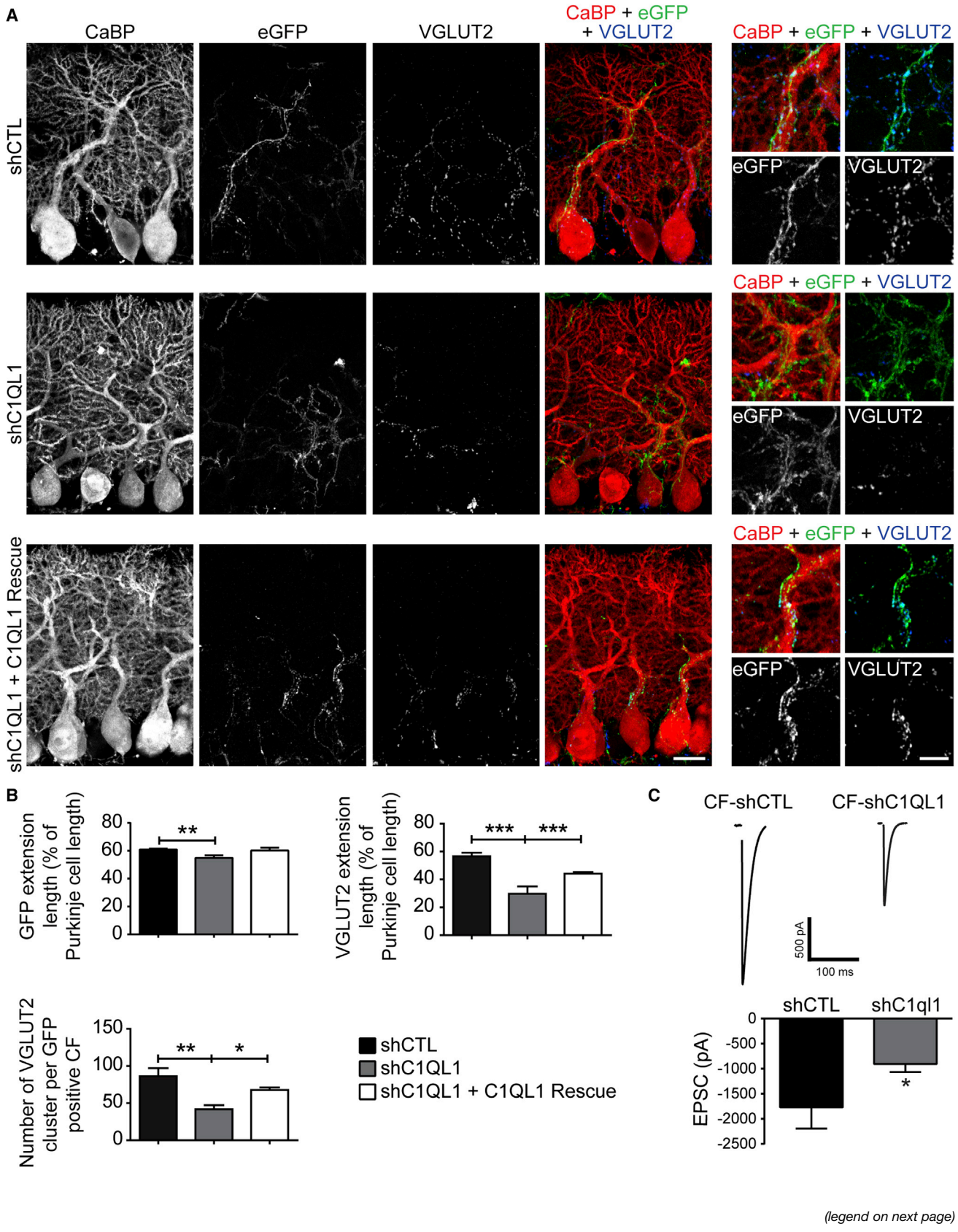

(legend on next page)

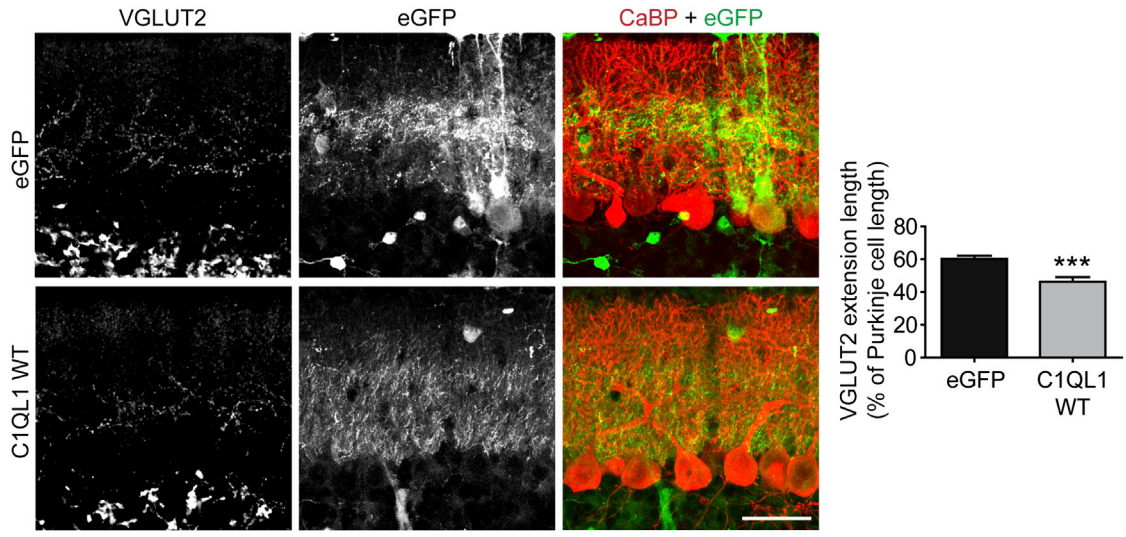

Figure 5. Misexpression of *C1ql1* Reduces the Synaptic Territory of CFs on PCs

C1ql1 misexpression in the cerebellum was performed using stereotaxic injections in the vermis of P7 mice of lentiviral particles, driving the expression of GFP (eGFP) alone or together with C1QL1 (C1QL1 WT). CF extension was imaged at P14 after immunostaining for VGLUT2 (CF synapses) and CaBP (entire PC). n = 6 animals per condition. Data are presented as mean ± SEM; unpaired Student's t test with Welch's correction; ***$p < 0.001$. The scale bar represents 40 μm.

elimination in the visual system (Stevens et al., 2007). Secretion of CBLN1 by granule cells is essential for the formation and stability of their synapses with PCs by bridging beta-neurexin and the glutamate receptor delta 2 (GluRδ2) (Hirai et al., 2005; Matsuda et al., 2010; Uemura et al., 2010). CBLN1 can also stimulate the maturation of presynaptic boutons to match the size of the postsynaptic density (Ito-Ishida et al., 2012). Our results now show that expression of C1QL1 by inferior olivary neurons and of its receptor BAI3 by the target PCs is necessary for the development of CF/PC synapses. Thus, the C1QL and CBLN subfamilies play similar and essential roles during brain development by promoting synaptogenesis between neurons that secrete them and target neurons that express their receptors. Their distinct and non-overlapping expression patterns ensure proper connectivity between different neuronal populations, suggesting that C1QL and CBLN subfamilies are part of the potential "chemoaffinity code" contributing to synapse specificity during circuit formation (Sanes and Yamagata, 2009; Sperry, 1963).

Interestingly, these two subfamilies of complement C1Q-related proteins have distinct types of receptors, both at the structural and functional level: the BAI3 receptor is an adhesion-GPCR that binds C1QL proteins and controls RAC1 activation, whereas GluRδ2, the receptor for CBLN1, has a structure homologous to the glutamate ionotropic receptors and is coupled intracellularly to various signaling molecules such as PDZ proteins or the protein phosphatase PTPMEG (Yuzaki, 2012). GluRδ2 becomes restricted to the PF/PC synapses after P14 and is necessary for synapse formation and maintenance between PFs and PCs. Its removal in genetically modified mice decreases the number of PF/PC synapses and consequently increases the synaptic territory of CFs (Uemura et al., 2007). Thus, each excitatory input of PCs is characterized by a member of a specific C1Q-related subfamily that controls synaptogenesis on PCs through a different signaling pathway. Both GluRδ2 and BAI3 receptors are expressed early in PCs and remain highly expressed in the adult: whether and how these two signaling pathways functionally interact to regulate synaptogenesis remains to be determined.

The subcellular localization of synapses between different types of inputs on a given target neuron is precisely controlled. For example, PFs contact PCs on spines of distal dendrites, whereas CFs make their synapses on proximal dendrites. What regulates this level of specificity, essential for proper integration of signals in the brain, is poorly understood. Adhesion

Figure 4. The C1QL1 Protein from Inferior Olivary Neurons Promotes CF/PC Synaptogenesis

(A) Defects in CF/PC synapses were assessed at P14 after *C1ql1* knockdown. Stereotaxic injections of recombinant lentiviral particles driving expression of a shRNA against *C1ql1* (shC1QL1), a control shRNA (shCTL), or shC1QL1 together with a *C1ql1* rescue cDNA were performed in the inferior olive of P4 mice. Immunostaining for VGLUT2 antibody was used to visualize CF synapses. eGFP-positive CFs correspond to transduced inferior olivary neurons. The scale bar in the left panel represents 20 μm and in the right panel represents 10 μm.

(B) Extension of CFs (eGFP) or of CF synapses (VGLUT2) relative to PC height, as well as the number of CF synapses, were quantified using Image J. n = 4–8 animals and $n \geq 95$ CFs per condition. Data are presented as mean ± SEM; one-way ANOVA followed by Kruskal-Wallis post hoc test or Dunn's test; *$p < 0.05$; **$p < 0.01$; ***$p < 0.001$.

(C) Top CF-induced EPSCs recorded in PCs located in the target zone of virally transduced CFs (cf. text). Bottom panel: summary bar graphs showing the averaged peak amplitude of CF-EPSCs for each condition. Bars represent mean ± SEM values. Mann Whitney *U* test; *$p < 0.05$.

See also Figure S6.

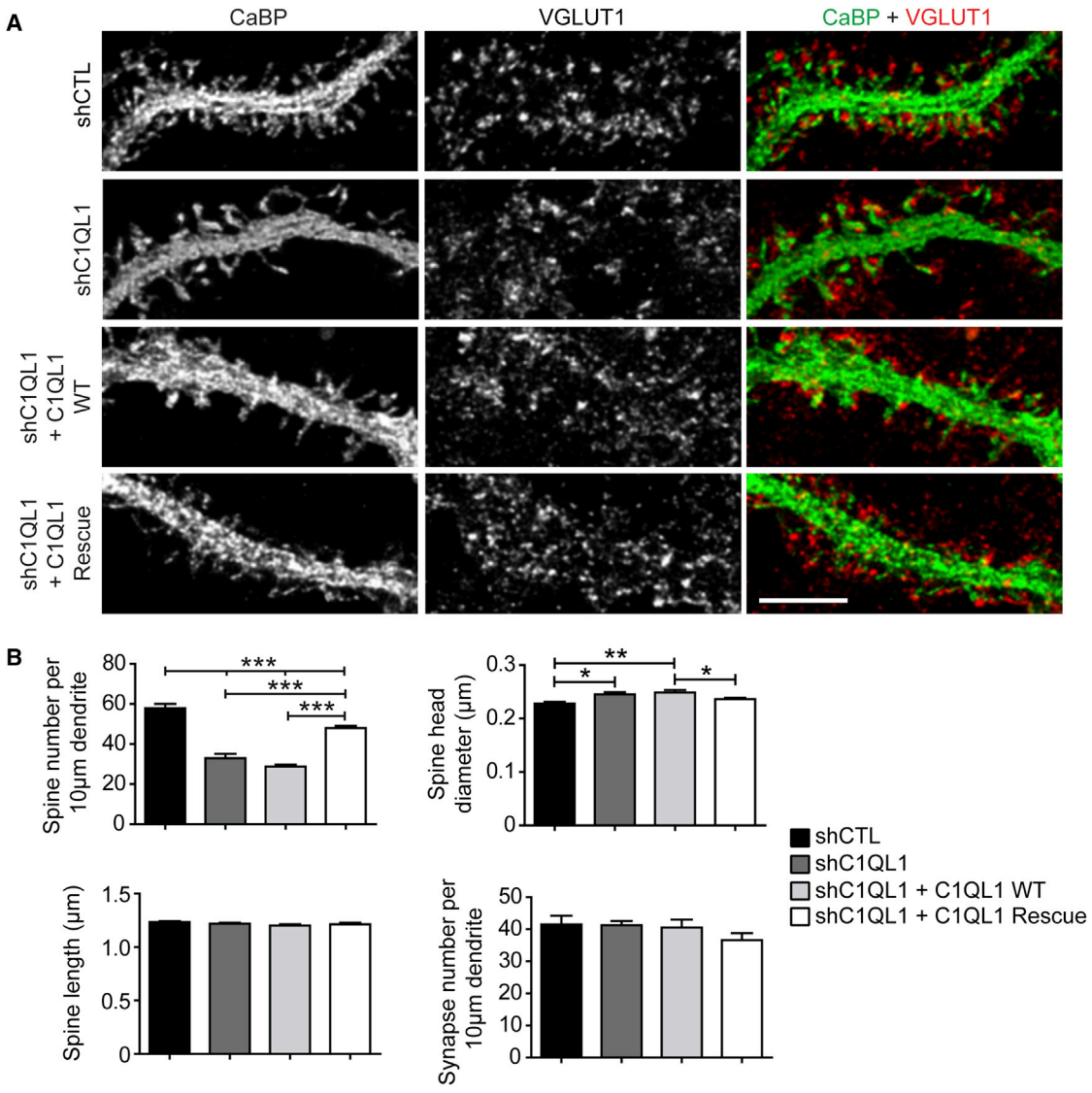

Figure 6. Transient C1QL1 Secretion in the Cerebellum Promotes PC Spinogenesis

(A) The role of cerebellar C1QL1 was assessed in mixed cultures using an RNAi approach. Neurons were transduced at DIV4 with recombinant lentiviral particles driving expression of control shRNA (shCTL) or shC1QL1, a mixture of recombinant lentiviral particles driving either shC1QL1 space and wild-type *C1ql1* (knockdown condition), or shC1QL1 and *C1ql1 Rescue* cDNA (control condition). High-resolution confocal imaging was performed at DIV14 after immunostaining for calbindin (CaBP) and VGLUT1 (specific for PF synapses). The scale bar represents 5 µm.

(B) Effects of *C1ql1* knockdown on spine density, head diameter, and length, as well as on the number of VGLUT1 synaptic contacts were quantified. n ≥ 30 cells, three to four independent experiments. Data are presented as mean ± SEM; one-way ANOVA followed by Newman-Keuls or Kruskal-Wallis post hoc test; *p < 0.05; **p < 0.01; ***p < 0.001. Spine density was significantly reduced in all conditions when compared to the shCTL condition.

See also Figure S3B.

proteins have been involved, such as cadherin-9 for excitatory synapses in the hippocampus (Williams et al., 2011) or L1 family proteins for inhibitory synapses in cerebellar PCs (Ango et al., 2004). Studies of mutant mouse models, together with experiments involving lesions or modulation of activity, have demonstrated that PFs and CFs compete to establish their non-overlapping innervation pattern on cerebellar PCs (Cesa and Strata, 2009; Rossi and Strata, 1995). Whereas PF/PC synaptogenesis has already begun on the developing dendrites, a single CF starts translocating at P9 on the PC primary dendrite (Hashimoto et al., 2009). These data suggest an active mechanism for the control of CF translocation and synaptic territory. *C1ql1* expression highly increases in inferior olivary neurons and becomes restricted to CFs in the olivocerebellar network starting at P7. Removing either C1QL1 from inferior olivary neurons or BAI3 from PCs or misexpressing *C1ql1* in the cerebellum during postnatal development reduces the extent of the synaptic territory of CFs on their target PCs, showing that the

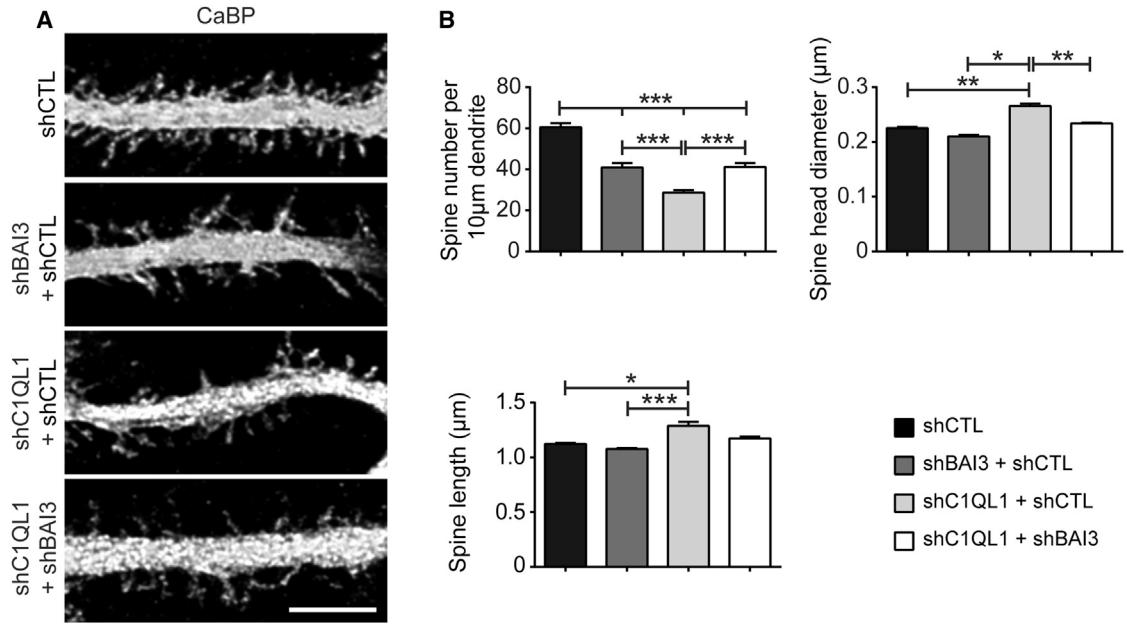

Figure 7. The Modulation by C1QL1 of PC Spinogenesis Depends on Normal Levels of the BAI3 Receptor

(A) The functional interaction between C1QL1 and BAI3 was assessed by simultaneous reduction of their expression in cerebellar cultures using an RNAi approach. Neurons were transduced at DIV4 with a mixture of recombinant lentiviral particles driving either shC1QL1 and shBAI3 (double knockdown), shBAI3 and shCTL (*Bai3* knockdown alone), shC1QL1 and shCTL (*C1ql1* knockdown alone), or double amounts of shCTL. Analysis was performed using high-resolution confocal imaging at DIV14 after immunostaining for calbindin (CaBP). The scale bar represents 5 µm.

(B) Quantitative analysis of spine density performed using Neuron Studio. n ≥ 30 cells, three to four independent experiments (data are presented as mean ± SEM; one-way ANOVA followed by Newman-Keuls post hoc test; *p < 0.05; **p < 0.01; ***p < 0.001). Spine density was significantly reduced in all conditions when compared to the shCTL condition.

secreted protein C1QL1 and its receptor the adhesion-GPCR BAI3 promote CF synaptic territory. The adhesion-GPCR BAI3 is also located at PF/PC synapses and modulates the number of distal dendritic spines where those synapses are formed. Thus, the proper territory of innervation on PCs could be controlled by the competition of excitatory afferents for a limited amount of BAI3 receptor sites. A deficient C1QL1/BAI3 pathway is not enough to prevent CF translocation (Figures 2 and 4) and does not induce PF invasion of the CF territory (data not shown). Eph receptor signaling has been shown to prevent invasion of the CF territory by PFs given that its deficit induces spinogenesis and PF synaptogenesis in the proximal dendrites (Cesa et al., 2011). Thus, CF synaptogenesis and translocation on PCs are controlled by different signaling pathways during development.

The C1QL/BAI3 signaling pathway might regulate synapse specificity in multiple neuronal populations that display segregation of synaptic inputs. In the hippocampus, mossy fibers from the dentate gyrus connect pyramidal cells on thorny excrescences close to the soma, whereas entorhinal afferents form their contacts on distal portions of the dendrites. *C1ql3* is expressed by granule cells in the dentate gyrus and could thus control the segregation pattern of inputs on the dendritic tree of hippocampal pyramidal cells through interaction with the BAI3 receptor. Recently, the importance of secreted proteins in defining synapse specificity has also been highlighted in the invertebrate nervous system by the study of Ce-Punctin (Pinan-Lucarré et al., 2014). Thus, the timely and restricted expression of secreted ligands and their interaction with receptors that regulate spinogenesis, synaptogenesis, and synaptic territory constitute a general mechanism that coordinates the development of a specific and functional neuronal connectivity.

EXPERIMENTAL PROCEDURES

All animal protocols and animal facilities were approved by the Comité Régional d'Ethique en Expérimentation Animale (no. 00057.01) and the veterinary services (C75 05 12).

cDNA and RNAi Constructs

The shRNA sequences were 5′tcgtcatagcgtgcatagg3′ for CTL, 5′ggtgaag ggagtcatttat3′ for *Bai3*, and 5′ggcaagtttacatgcaaca3′ for *C1ql1*. They were subcloned under the control of the H1 promoter in a lentiviral vector that also drives *eGFP* expression under the control of PGK1 promoter (Avci et al., 2012). The *C1ql1 WT* cDNA construct (mouse clone no. BC118980) was cloned into the lentiviral vector pSico (Addgene) under the control of the PGK1 promoter. The *eGFP* sequence of the original pSico was replaced by the cerulean sequence. The *C1ql1 Rescue* is a mutated form of *C1ql1 WT* with three nucleotide changes (T498C, A501C, and C504T) that do not modify the amino acid sequence.

In Vivo Injections

Injections of lentiviral particles in the cerebellum were performed in the vermis of anesthetized P7 Swiss mice at a 1.25-mm depth from the skull to target the molecular and PC layers and at 1.120 mm for Figure 5. Injections of lentiviral particles in the inferior olive were performed in anesthetized P4 Swiss mice, on the left side of the basilar artery in the brainstem. Calibration of the

Please cite this article in press as: Sigoillot et al., The Secreted Protein C1QL1 and Its Receptor BAI3 Control the Synaptic Connectivity of Excitatory Inputs Converging on Cerebellar Purkinje Cells, Cell Reports (2015), http://dx.doi.org/10.1016/j.celrep.2015.01.034

injections showed that this procedure led to transduction of parts of the principal and dorsal accessory olive. 0.5–1 μl of lentivirus was injected per animal using pulled calibrated pipets.

Dendritic Spine and Synapse Analysis

For each PC, a dendritic segment of about 100 μm in length and in the distal part of the arborization or after the second branching point was considered. Dendritic spines were analyzed with the NeuronStudio software (version 9.92; Rodriguez et al., 2008). The spine head diameter corresponds to the minimal diameter of the ellipse describing the spine head, calculated in the xy axis. The spine length is the distance from the "tip" of the spine to the surface of the model. Minimum height was set to 0.5 μm and maximum to 8 μm. Synaptic contacts were analyzed using ImageJ-customized macro. The CaBP and the VGLUT1 objects found above a user-defined threshold were selected. Image calculator was used to extract the signal common to CaBP and VGLUT1 images: the number and volume of these puncta were quantified with the 3D Object counter plugin from ImageJ. The size of presynaptic VGLUT2 clusters was analyzed using the ImageJ plugin 3D object counter. Bin number of VGLUT2 cluster intersection was assessed using the Advanced Scholl analysis plugin from ImageJ.

Statistical Analysis

Data generated with NeuronStudio or ImageJ were imported in GraphPad Prism for statistical analysis. Data were analyzed by averaging the values for each neuron in each condition. Values are given as mean ± SEM. Student's t test or one-way ANOVA followed by Newman-Keuls post hoc test were performed for comparison of two or more samples, respectively. When distribution did not fit the Normal law (assessed using Graphpad Prism), Mann-Whitney *U* test or one-way ANOVA followed by Kruskal-Wallis post hoc test were used. Two-way ANOVA followed by Bonferroni post hoc test was performed for the analysis of bin number of VGLUT2. *$p < 0.05$; **$p < 0.01$; ***$p < 0.001$.

Supplemental Experimental Procedures (cerebellar mixed cultures, qRT-PCR, in situ hybridization, immunohistochemistry, image acquisition, and electrophysiology) are available online.

SUPPLEMENTAL INFORMATION

Supplemental Information includes Supplemental Experimental Procedures and seven figures and can be found with this article online at http://dx.doi.org/10.1016/j.celrep.2015.01.034.

AUTHOR CONTRIBUTIONS

F.S., S.M.S., and P.I. designed the experiments. S.M.S., K.I., F.B., I.G.-C., and M.T. performed experiments. G.V. provided critical reagents. All authors discussed the data. F.S., S.M.S., and P.I. wrote the manuscript.

ACKNOWLEDGMENTS

We would like to thank Pr. A. Prochiantz for critical reading of the manuscript; Dr. M. Wassef for help with in situ hybridization and inferior olive injections; J. Teillon, N. Quenech'du, and P. Mailly from the CIRB Imaging Facility; and J.-C. Graziano from the CIRB Animal Facility. This work has received support under the Investissements d'Avenir program launched by the French government and implemented by the ANR with the references ANR-10-LABX-54 MEMO LIFE (to S.M.S. and F.S.) and ANR-11-IDEX-0001-02 PSL* Research University (to I.G.-C. and F.S.) and under the TIGER project funded by INTERREG IV Rhin Supérieur program and European Funds for Regional Development (FEDER; nos. A31, FB, and PI). Funding was also provided by Fondation Bettencourt Schuller, CNRS, NeRF Ile de France (to S.M.S.), Ecole des Neurosciences de Paris (to K.I.), Fondation pour la Recherche Médicale (to M.T.), ATIP AVENIR (to F.S.), Fondation Jérôme Lejeune (to F.S.), Association Française pour le Syndrôme de Rett (to F.S.), ANR-2010-JCJC-1403-1 (to P.I.), and ANR-13-SAMA-0010-01 (to F.S.).

Received: July 29, 2014
Revised: January 8, 2015
Accepted: January 15, 2015
Published: February 5, 2015

REFERENCES

Ango, F., di Cristo, G., Higashiyama, H., Bennett, V., Wu, P., and Huang, Z.J. (2004). Ankyrin-based subcellular gradient of neurofascin, an immunoglobulin family protein, directs GABAergic innervation at purkinje axon initial segment. Cell *119*, 257–272.

Ango, F., Wu, C., Van der Want, J.J., Wu, P., Schachner, M., and Huang, Z.J. (2008). Bergmann glia and the recognition molecule CHL1 organize GABAergic axons and direct innervation of Purkinje cell dendrites. PLoS Biol. *6*, e103.

Avci, H.X., Lebrun, C., Wehrlé, R., Doulazmi, M., Chatonnet, F., Morel, M.-P., Ema, M., Vodjdani, G., Sotelo, C., Flamant, F., and Dusart, I. (2012). Thyroid hormone triggers the developmental loss of axonal regenerative capacity via thyroid hormone receptor α1 and krüppel-like factor 9 in Purkinje cells. Proc. Natl. Acad. Sci. USA *109*, 14206–14211.

Bolliger, M.F., Martinelli, D.C., and Südhof, T.C. (2011). The cell-adhesion G protein-coupled receptor BAI3 is a high-affinity receptor for C1q-like proteins. Proc. Natl. Acad. Sci. USA *108*, 2534–2539.

Cesa, R., and Strata, P. (2009). Axonal competition in the synaptic wiring of the cerebellar cortex during development and in the mature cerebellum. Neuroscience *162*, 624–632.

Cesa, R., Premoselli, F., Renna, A., Ethell, I.M., Pasquale, E.B., and Strata, P. (2011). Eph receptors are involved in the activity-dependent synaptic wiring in the mouse cerebellar cortex. PLoS ONE *6*, e19160.

Collins, M.O., Husi, H., Yu, L., Brandon, J.M., Anderson, C.N.G., Blackstock, W.P., Choudhary, J.S., and Grant, S.G.N. (2006). Molecular characterization and comparison of the components and multiprotein complexes in the postsynaptic proteome. J. Neurochem. *97* (1), 16–23.

DeRosse, P., Lencz, T., Burdick, K.E., Siris, S.G., Kane, J.M., and Malhotra, A.K. (2008). The genetics of symptom-based phenotypes: toward a molecular classification of schizophrenia. Schizophr. Bull. *34*, 1047–1053.

Duman, J.G., Tzeng, C.P., Tu, Y.-K., Munjal, T., Schwechter, B., Ho, T.S.-Y., and Tolias, K.F. (2013). The adhesion-GPCR BAI1 regulates synaptogenesis by controlling the recruitment of the Par3/Tiam1 polarity complex to synaptic sites. J. Neurosci. *33*, 6964–6978.

Hashimoto, K., Ichikawa, R., Kitamura, K., Watanabe, M., and Kano, M. (2009). Translocation of a "winner" climbing fiber to the Purkinje cell dendrite and subsequent elimination of "losers" from the soma in developing cerebellum. Neuron *63*, 106–118.

Hirai, H., Pang, Z., Bao, D., Miyazaki, T., Li, L., Miura, E., Parris, J., Rong, Y., Watanabe, M., Yuzaki, M., and Morgan, J.I. (2005). Cbln1 is essential for synaptic integrity and plasticity in the cerebellum. Nat. Neurosci. *8*, 1534–1541.

Iijima, T., Miura, E., Watanabe, M., and Yuzaki, M. (2010). Distinct expression of C1q-like family mRNAs in mouse brain and biochemical characterization of their encoded proteins. Eur. J. Neurosci. *31*, 1606–1615.

Ito-Ishida, A., Miyazaki, T., Miura, E., Matsuda, K., Watanabe, M., Yuzaki, M., and Okabe, S. (2012). Presynaptically released Cbln1 induces dynamic axonal structural changes by interacting with GluD2 during cerebellar synapse formation. Neuron *76*, 549–564.

Lanoue, V., Usardi, A., Sigoillot, S.M., Talleur, M., Iyer, K., Mariani, J., Isope, P., Vodjdani, G., Heintz, N., and Selimi, F. (2013). The adhesion-GPCR BAI3, a gene linked to psychiatric disorders, regulates dendrite morphogenesis in neurons. Mol. Psychiatry *18*, 943–950.

Liao, H.-M., Chao, Y.-L., Huang, A.-L., Cheng, M.-C., Chen, Y.-J., Lee, K.-F., Fang, J.-S., Hsu, C.-H., and Chen, C.-H. (2012). Identification and characterization of three inherited genomic copy number variations associated with familial schizophrenia. Schizophr. Res. *139*, 229–236.

Luo, L. (2002). Actin cytoskeleton regulation in neuronal morphogenesis and structural plasticity. Annu. Rev. Cell Dev. Biol. *18*, 601–635.

Matsuda, K., Miura, E., Miyazaki, T., Kakegawa, W., Emi, K., Narumi, S., Fukazawa, Y., Ito-Ishida, A., Kondo, T., Shigemoto, R., et al. (2010). Cbln1 is a ligand for an orphan glutamate receptor delta2, a bidirectional synapse organizer. Science *328*, 363–368.

O'Rourke, N.A., Weiler, N.C., Micheva, K.D., and Smith, S.J. (2012). Deep molecular diversity of mammalian synapses: why it matters and how to measure it. Nat. Rev. Neurosci. *13*, 365–379.

Okajima, D., Kudo, G., and Yokota, H. (2011). Antidepressant-like behavior in brain-specific angiogenesis inhibitor 2-deficient mice. J. Physiol. Sci. *61*, 47–54.

Park, D., Tosello-Trampont, A.-C., Elliott, M.R., Lu, M., Haney, L.B., Ma, Z., Klibanov, A.L., Mandell, J.W., and Ravichandran, K.S. (2007). BAI1 is an engulfment receptor for apoptotic cells upstream of the ELMO/Dock180/Rac module. Nature *450*, 430–434.

Pinan-Lucarré, B., Tu, H., Pierron, M., Cruceyra, P.I., Zhan, H., Stigloher, C., Richmond, J.E., and Bessereau, J.-L. (2014). C. elegans Punctin specifies cholinergic versus GABAergic identity of postsynaptic domains. Nature *511*, 466–470.

Rodriguez, A., Ehlenberger, D.B., Dickstein, D.L., Hof, P.R., and Wearne, S.L. (2008). Automated three-dimensional detection and shape classification of dendritic spines from fluorescence microscopy images. PLoS ONE *3*, e1997.

Rossi, F., and Strata, P. (1995). Reciprocal trophic interactions in the adult climbing fibre-Purkinje cell system. Prog. Neurobiol. *47*, 341–369.

Salinas, P.C. (2012). Wnt signaling in the vertebrate central nervous system: from axon guidance to synaptic function. Cold Spring Harb. Perspect. Biol. *4*, a008003.

Sanes, J.R., and Yamagata, M. (2009). Many paths to synaptic specificity. Annu. Rev. Cell Dev. Biol. *25*, 161–195.

Selimi, F., Cristea, I.M., Heller, E., Chait, B.T., and Heintz, N. (2009). Proteomic studies of a single CNS synapse type: the parallel fiber/purkinje cell synapse. PLoS Biol. *7*, e83.

Shen, K., and Scheiffele, P. (2010). Genetics and cell biology of building specific synaptic connectivity. Annu. Rev. Neurosci. *33*, 473–507.

Sia, G.-M., Béïque, J.-C., Rumbaugh, G., Cho, R., Worley, P.F., and Huganir, R.L. (2007). Interaction of the N-terminal domain of the AMPA receptor GluR4 subunit with the neuronal pentraxin NP1 mediates GluR4 synaptic recruitment. Neuron *55*, 87–102.

Sotelo, C. (1990). Cerebellar synaptogenesis: what we can learn from mutant mice. J. Exp. Biol. *153*, 225–249.

Sperry, R.W. (1963). Chemoaffinity in the orderly growth of nerve fiber patterns and connections. Proc. Natl. Acad. Sci. USA *50*, 703–710.

Stevens, B., Allen, N.J., Vazquez, L.E., Howell, G.R., Christopherson, K.S., Nouri, N., Micheva, K.D., Mehalow, A.K., Huberman, A.D., Stafford, B., et al. (2007). The classical complement cascade mediates CNS synapse elimination. Cell *131*, 1164–1178.

Südhof, T.C. (2008). Neuroligins and neurexins link synaptic function to cognitive disease. Nature *455*, 903–911.

Uemura, T., Kakizawa, S., Yamasaki, M., Sakimura, K., Watanabe, M., Iino, M., and Mishina, M. (2007). Regulation of long-term depression and climbing fiber territory by glutamate receptor delta2 at parallel fiber synapses through its C-terminal domain in cerebellar Purkinje cells. J. Neurosci. *27*, 12096–12108.

Uemura, T., Lee, S.-J., Yasumura, M., Takeuchi, T., Yoshida, T., Ra, M., Taguchi, R., Sakimura, K., and Mishina, M. (2010). Trans-synaptic interaction of GluRdelta2 and Neurexin through Cbln1 mediates synapse formation in the cerebellum. Cell *141*, 1068–1079.

Williams, M.E., Wilke, S.A., Daggett, A., Davis, E., Otto, S., Ravi, D., Ripley, B., Bushong, E.A., Ellisman, M.H., Klein, G., and Ghosh, A. (2011). Cadherin-9 regulates synapse-specific differentiation in the developing hippocampus. Neuron *71*, 640–655.

Yamagata, M., and Sanes, J.R. (2008). Dscam and Sidekick proteins direct lamina-specific synaptic connections in vertebrate retina. Nature *451*, 465–469.

Yuste, R., and Bonhoeffer, T. (2004). Genesis of dendritic spines: insights from ultrastructural and imaging studies. Nat. Rev. Neurosci. *5*, 24–34.

Yuzaki, M. (2011). Cbln1 and its family proteins in synapse formation and maintenance. Curr. Opin. Neurobiol. *21*, 215–220.

Yuzaki, M. (2012). The ins and outs of GluD2—why and how Purkinje cells use the special glutamate receptor. Cerebellum *11*, 438–439.

Cell Reports

Supplemental Information

The Secreted Protein C1QL1 and Its Receptor BAI3 Control the Synaptic Connectivity of Excitatory Inputs Converging on Cerebellar Purkinje Cells

Séverine M. Sigoillot, Keerthana Iyer, Francesca Binda, Inés Gonzalez-Calvo, Maëva Talleur, Guilan Vodjdani, Philippe Isope, and Fekrije Selimi

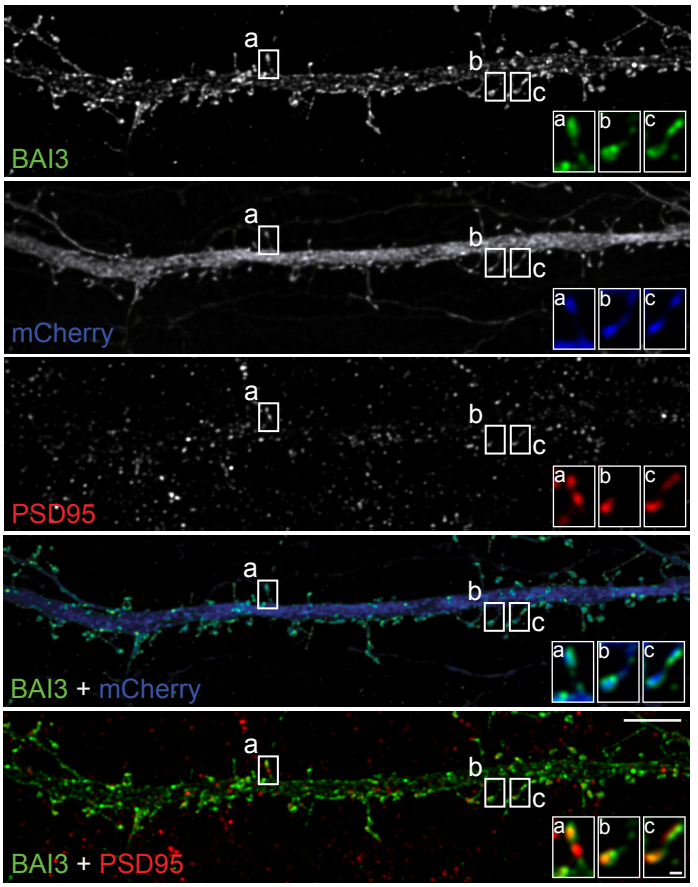

Figure S1, related to Figure 2 and 3. BAI3 is localized in spines and partially colocalized with the postsynaptic density in cultured hippocampal neurons. DIV20 hippocampal neurons co-transfected at DIV18 with BAI3 and mCherry constructs were immunostained for BAI3 and the postsynaptic density marker PSD95. Higher magnifications of regions (a-c) are shown in the insets on the bottom right. Scale bars, 5µm and 0.5µm for insets.

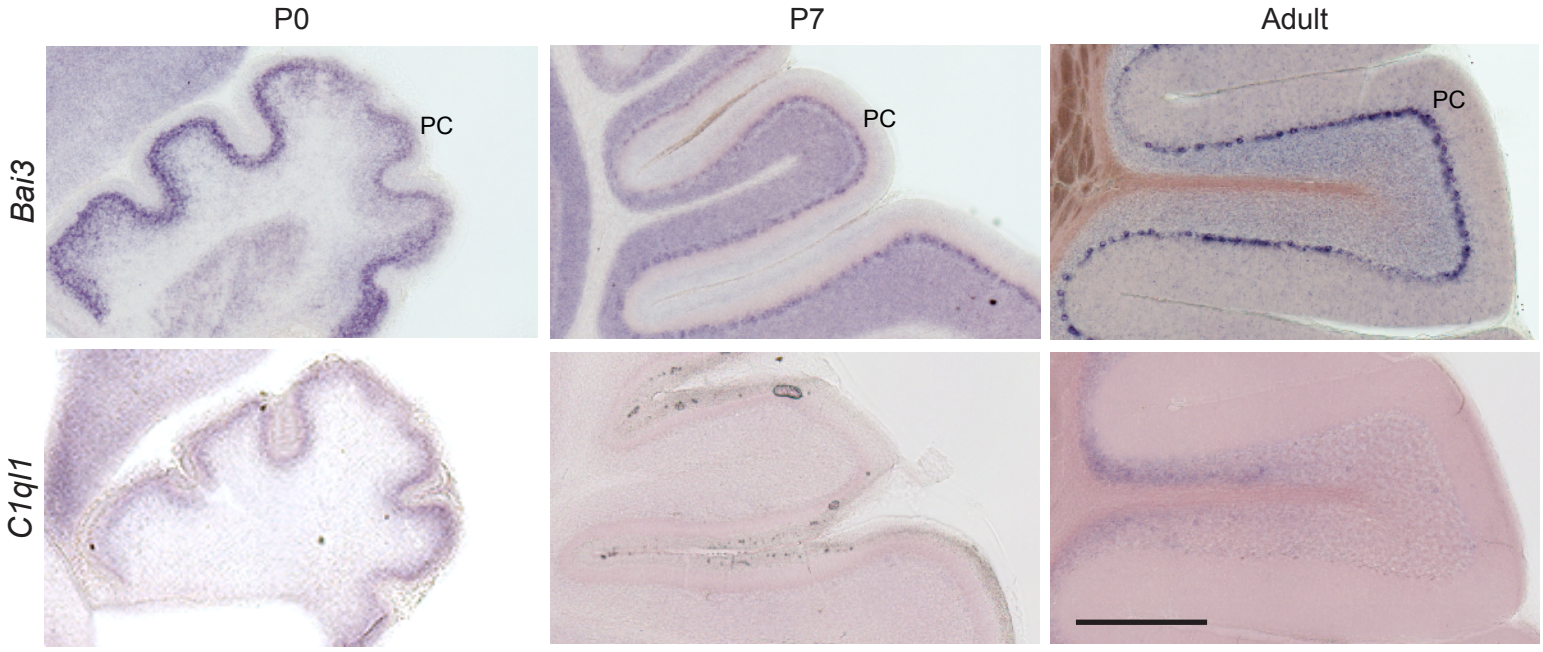

Figure S2, related to Figure 1. *In situ* hybridization analysis of *Bai3* and *C1ql1* mRNA expression in the cerebellar cortex during postnatal development.
In situ hybridization experiments performed using a probe specific for *Bai3* or *C1ql1* on sagittal sections of mouse brain taken at postnatal day 0, 7 and adult. PC, Purkinje cell. Scale bar, 500μm.

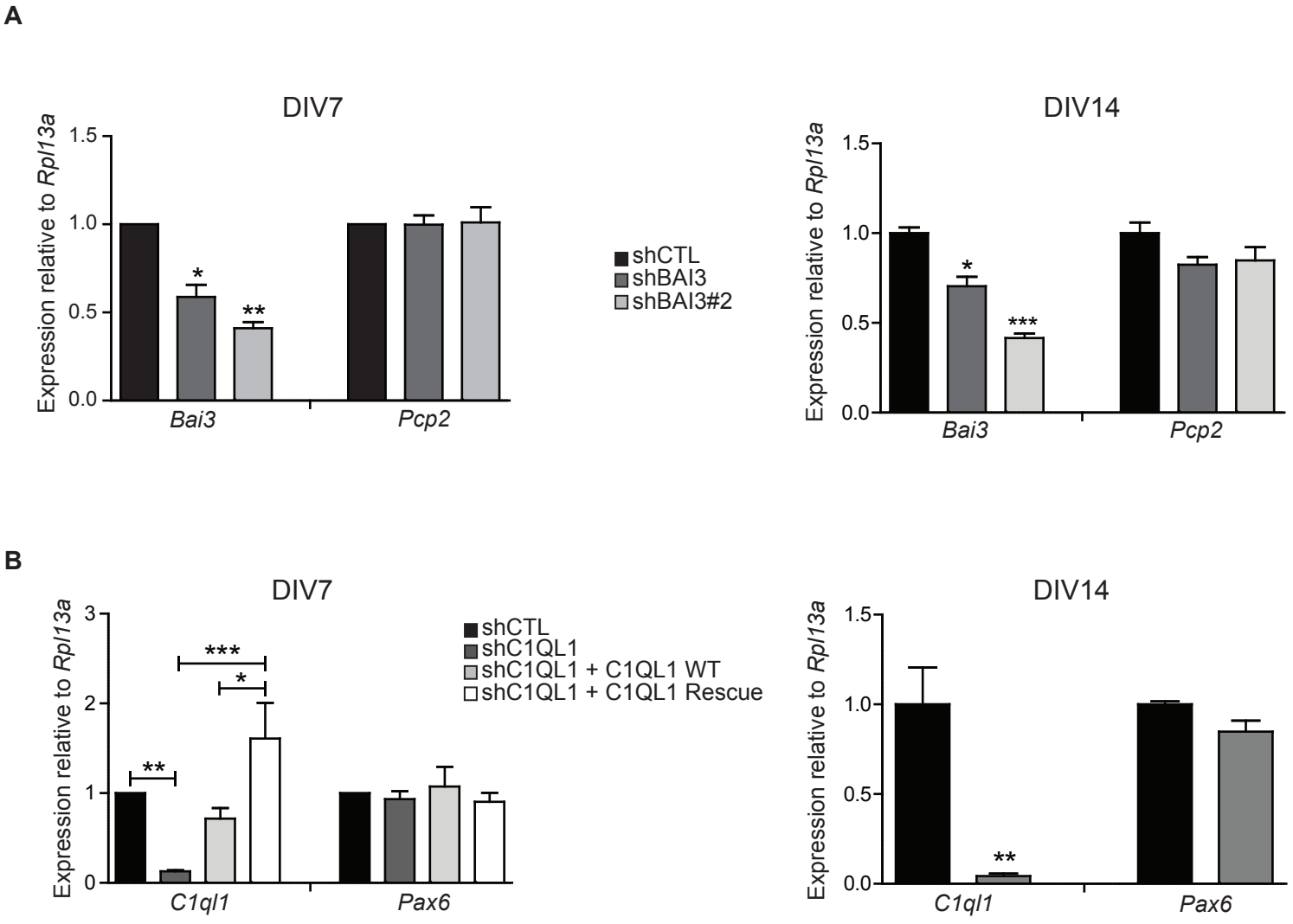

Figure S3, related to Figures 2, 3 and 6. Characterization of knockdown and rescue efficiency for our RNAi approach in cerebellar mixed cultures.

(A) Expression of *Bai3* and *Pcp2* mRNAs was assessed using quantitative RT-PCR on extracts from cerebellar mixed cultures. Transduction was performed at days in vitro 4 (DIV4) with lentiviruses driving the expression of two different shRNAs directed against *Bai3*, or the control shCTL and analysis at DIV7 (left) or DIV14 (right). Expression levels are normalized to the *Rpl13a* gene. Note that twice as many lentiviral particles are used for shBAI3#2. **(B)** Expression of *C1ql1* and *Pax6* mRNAs was assessed using quantitative RT-PCR on cerebellar mixed cultures at DIV7 or DIV14, respectively after 3 days or 10 days of transduction by lentiviruses driving the expression of a shRNA directed against *C1ql1* alone or in combination with lentiviruses expressing *C1ql1 WT* or *C1ql1 Rescue*, or the shCTL as control. Expression levels are normalized to the *Rpl13a* gene. N=3-7 independent experiments (Data are presented as mean ± SEM; One-way ANOVA followed by Newman-Keuls posthoc test, *$p < 0.05$, **$p < 0.01$, ***$p < 0.001$).

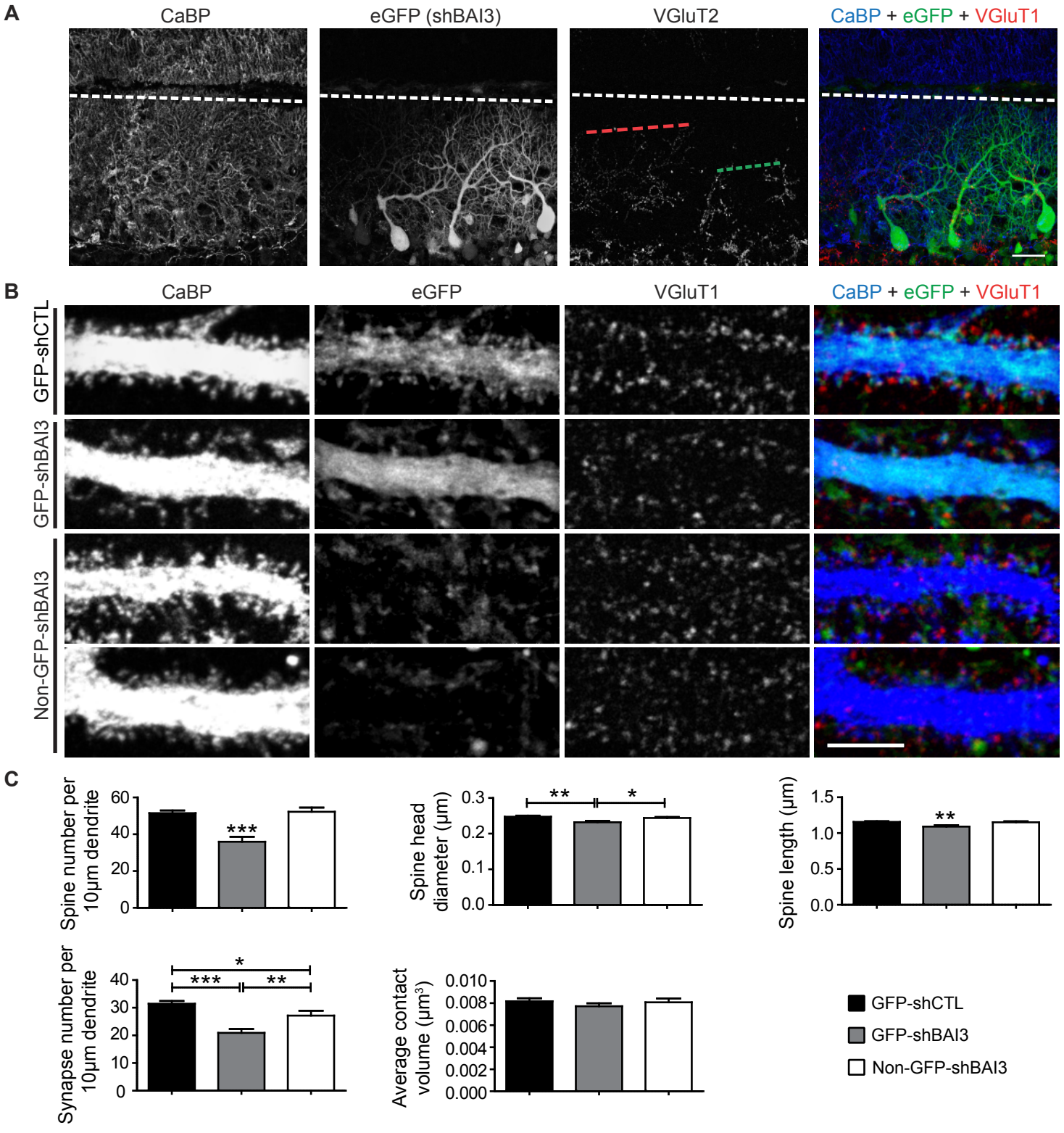

Figure S4, related to Figure 2 and 3. Cell autonomous role of BAI3 in Purkinje cells. (A) P21 immunostaining for vesicular glutamate transporter 2 antibody (VGluT2), a marker specific for climbing fiber synapses, on non-transduced PCs (GFP negative) or transduced PCs (GFP positive). Stereotaxic injections of recombinant lentiviral particles driving expression of a small hairpin RNA against *Bai3* (shBAI3) or control shRNA (shCTL) were performed at P7. Normal VGluT2 extension was observed in GFP-negative cells in contrast to the decreased extension visible on GFP-positive PCs. Granule cells are GFP-positives in the region of both GFP positive and negative cells. Pial surface: white dashed lines. Scale bar, 30µm. **(B)** Cerebellar mixed cultures were transduced at DIV4 with recombinant lentiviral particles driving expression of GFP together with a shRNA targeting *Bai3* (shBAI3) or a control shRNA (shCTL). Dendritic spines and parallel fiber synapses in transduced Purkinje cells (GFP) or non-transduced PCs (Non-GFP) were imaged at DIV14 after immunostaining for calbindin (CaBP) and vesicular glutamate transporter 1 antibody (VGluT1). Scale bar: 5µm. **(C)** Quantitative assessment of the number and morphology of spines was performed in cultured Purkinje cells using the NeuronStudio software. Quantitative assessment of the number and size of vGluT1 synaptic contacts was performed using ImageJ. N≥18 cells per condition, 3 independent experiments (Data are presented as mean ± SEM; One-way ANOVA followed by Newman-Keuls posthoc test, *p < 0.05; **p < 0.01; ***p < 0.001).

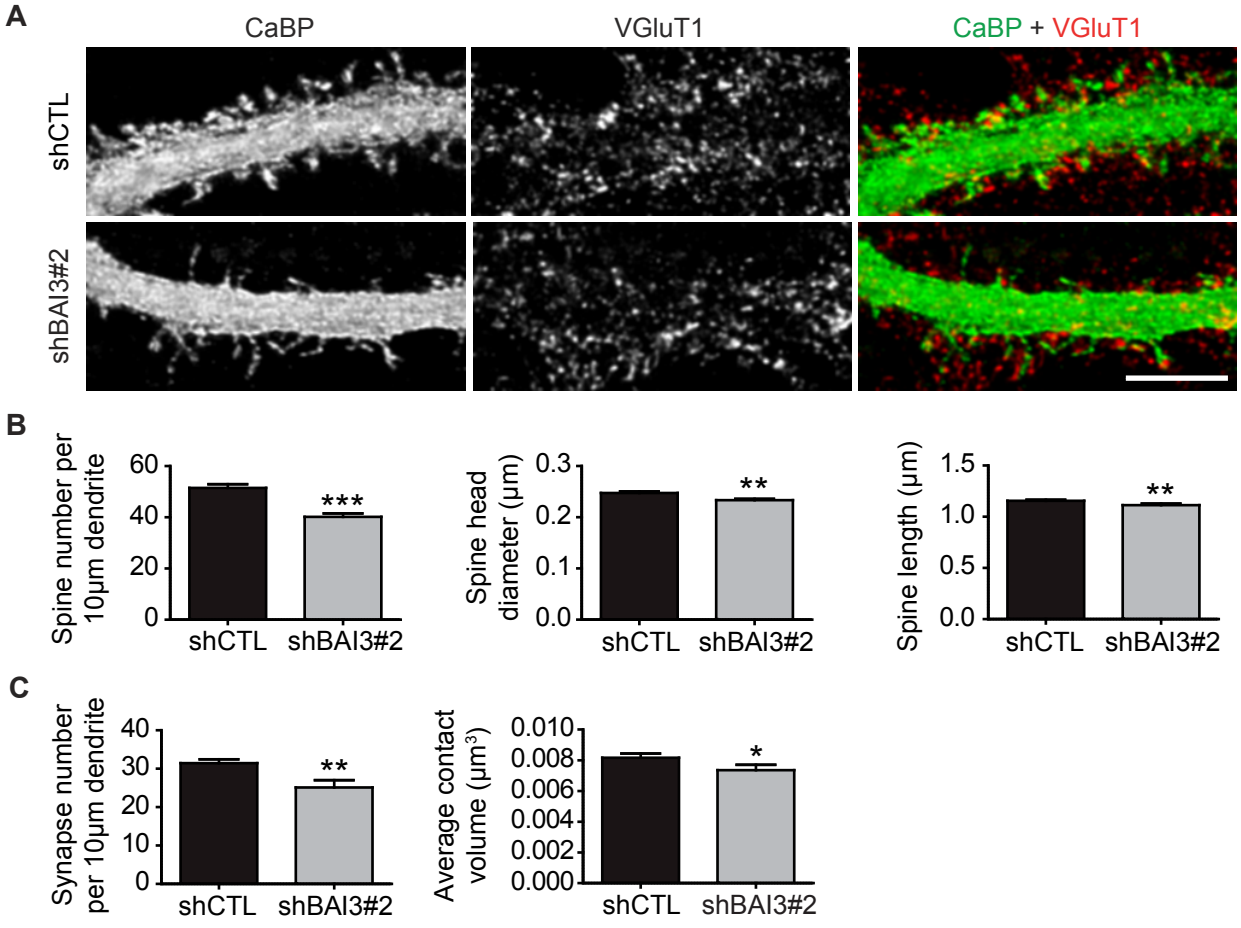

Figure S5, related to Figure 3. Data obtained with a second shRNA targeting BAI3 show similar effects on Parallel fiber/Purkinje cell spinogenesis and synaptogenesis in vitro. **(A)** Cerebellar mixed cultures were transduced at DIV4 with lentiviral particles driving expression of GFP together with a small hairpin RNA targeting *Bai3* (shBAI3#2) or a control shRNA (shCTL). Dendritic spines and parallel fiber synapses in transduced Purkinje cells (GFP positive) were imaged at DIV14 after immunostaining for calbindin (CaBP) and vesicular glutamate transporter 1 antibody (VGluT1), respectively. Scale bar: 5µm **(B)** Quantitative assessment of the number and morphology of Purkinje cell spines was performed using the NeuronStudio software. N≥40 cells per condition, 4 independent experiments (Data are presented as mean ± SEM; unpaired Student t test and Mann-Whitney *U* test for spine length, $^{**}p < 0.01$; $^{***}p < 0.001$). **(C)** Quantitative assessment of the number and size of vGluT1 synaptic contacts in DIV14 transduced Purkinje cells was performed using ImageJ. N≥40 cells per condition, 4 independent experiments (Data are presented as mean ± SEM; unpaired Student *t* test, $^{*}p < 0.05$; $^{**}p < 0.01$).

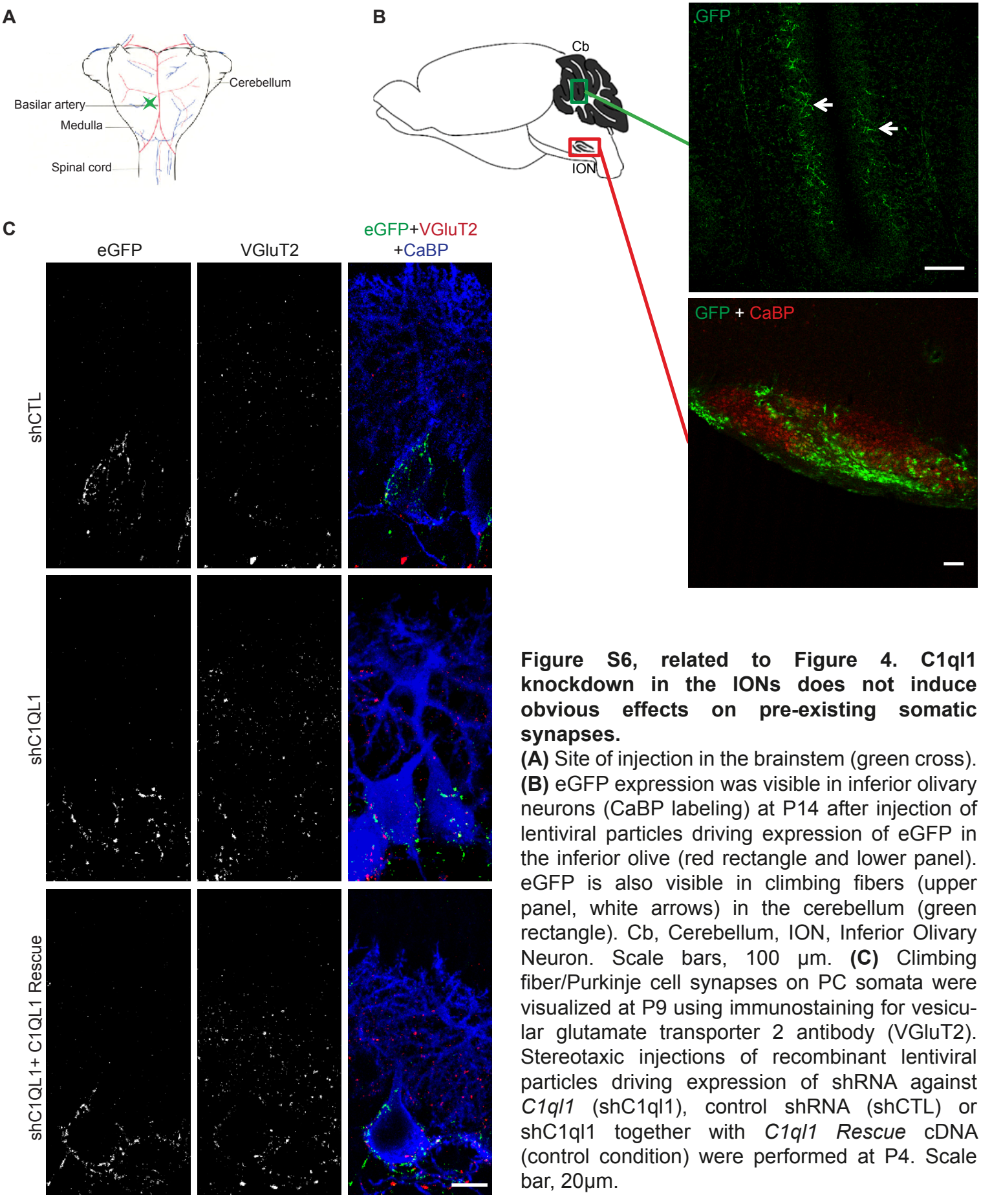

Figure S6, related to Figure 4. C1ql1 knockdown in the IONs does not induce obvious effects on pre-existing somatic synapses.

(A) Site of injection in the brainstem (green cross). **(B)** eGFP expression was visible in inferior olivary neurons (CaBP labeling) at P14 after injection of lentiviral particles driving expression of eGFP in the inferior olive (red rectangle and lower panel). eGFP is also visible in climbing fibers (upper panel, white arrows) in the cerebellum (green rectangle). Cb, Cerebellum, ION, Inferior Olivary Neuron. Scale bars, 100 µm. **(C)** Climbing fiber/Purkinje cell synapses on PC somata were visualized at P9 using immunostaining for vesicular glutamate transporter 2 antibody (VGluT2). Stereotaxic injections of recombinant lentiviral particles driving expression of shRNA against *C1ql1* (shC1ql1), control shRNA (shCTL) or shC1ql1 together with *C1ql1 Rescue* cDNA (control condition) were performed at P4. Scale bar, 20µm.

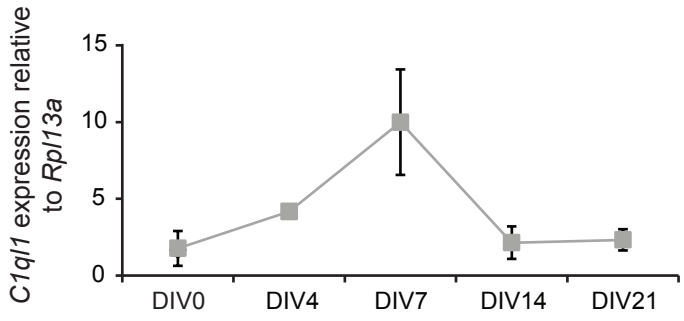

Figure S7, related to Figure 1. *C1ql1* expression in cerebellar cultures.
Expression of *C1ql1* was assessed at different stages of cerebellar culture development using quantitative RT-PCR on cell extracts (days in vitro, DIV0 to 21). Expression levels are normalized to the *Rpl13a* gene. N=2 samples per stage. Data are presented as mean ± SEM.

-Supplemental Experimental Procedures

cDNA and RNAi constructs

The *BAI3-WT* construct was cloned into the pEGFP-C2 vector from mouse cDNA clone #BC099951. The shRNA #2 sequence for BAI3 was: 5'tgcagaatttacccttga3', and was subcloned under the H1 promoter in a lentiviral vector that also drives eGFP expression (Avci et al., 2012).

RTqPCR

RNA samples were obtained from mixed cerebellar cultures using the RNeasy Mini kit (QIAGEN, Hilden, Germany), cDNA were amplified using the SuperScript® VILO™ cDNA Synthesis kit (Life technologies, Paisley, UK) according to manufacturer's instructions. Quantitative PCR was performed using the TaqMan Universal Master Mix II with UNG (Applied Biosystems, Courtaboeuf, France) and the following TaqMan probes: *Bai3* (#4331182_Mm00657451_m1), *C1ql1* (#4331182_Mm00657289_m1), *Rpl13a* (#4331182_Mm01612986_gH), *Pcp2* (#4331182_Mm00435514_m1), *Pax6* (#4331182_Mm00443081_m1).

In situ Hybridization

In situ hybridization was performed using a previously described protocol with minor modifications (Bally-Cuif et al., 1992). Briefly, paraformaldehyde-fixed freely floating vibratome sections were obtained (100 µm thickness) from mouse brains at postnatal day 0 (P0), P7 and adult (more than 6 weeks). The probe sequences corresponded to the following nucleotide residues for the indicated mouse cDNA: 3955-4708 bp for *Bai3* (NM_175642.4), 641-1200 bp for *C1ql1* (NM_011795.2) and 501-1017 bp for *C1ql3* (NM_153155.2). The riboprobes were used at a final concentration of 2 µg/µL. The proteinase K (10µg/mL)

treatment was given for 30 seconds for P0 and P7 brain sections, and 10 minutes for adult brain sections. The anti-digoxigenin-AP antibody was used at a dilution of 1/2000.

Primary neuronal cultures

Cerebellar mixed cultures were prepared from P0 Swiss mouse cerebella and were dissected and dissociated according to previously published protocol (Tabata et al., 2000). Neurons were seeded at a density of $5x10^6$ cells/ml. Hippocampal cultures were prepared from E18 Swiss mouse embryos as previously published with minor modifications (Fath et al., 2008). Hippocampal neurons were transfected at DIV18 using Lipofectamine-2000 (Life technologies, Carlsbad, USA) according to the manufacturer's protocol.

Immunocytochemistry, immunohistochemistry and antibodies

Immunostaining was performed on cells fixed with 2% paraformaldehyde in PBS or on 30 micrometer thick sagittal cerebellar sections obtained using a freezing microtome from brains of mice perfused with 4% paraformaldehyde in PBS. The following antibodies were used: anti-CaBP mouse antibody (Swant, Marly, Switzerland, #300), anti-VGluT1 guinea pig antibody (Millipore, Molsheim, France, #AB5905), anti-VGluT2 guinea pig antibody (Millipore, Molsheim, France, #AB2251), anti-BAI3 rabbit antibody (Sigma, St Louis, USA, #HPA015963) and anti-PSD95 rabbit antibody (Cell signaling, Leiden, The Netherlands, #3450).

Image acquisition and analysis

Image stacks were acquired using a Confocal Microscope (SP5, Leica), using either 40x (1.25 NA, oil immersion, pixel size: 211 nm and 144 nm for vGluT2 extension in shBAI3 and C1QL1 misexpression experiments, respectively) or 63x (1.4 NA, oil immersion, pixel size: 57 nm for *in vitro* imaging, pixel size: 38 nm for *in vivo* imaging of vGluT2 staining) or 20X (0.7 NA, pixel size 60 nm for hippocampal neurons) objectives. The pinhole aperture was set

to 1 Airy Unit and a z-step of 200 nm was used. Laser intensity and photomultiplier tube (PMT) gain was set so as to occupy the full dynamic range of the detector. Images were acquired in 16-bit range. For spine and synapse analysis, deconvolution was performed with Huygens 4.1 software (Scientific Volume Imaging) using Maximum Likelihood Estimation algorithm. 40 iterations were applied in classical mode, background intensity was averaged from the voxels with lowest intensity, and signal to noise ratio values were set to a value of 25.

Electrophysiology

Responses to parallel (PF) and climbing fibers (CF) stimulation were recorded in Purkinje cells in acute cerebellar slices from Swiss mice (P18 to P23) after lentivirus injection at P7 in the cerebellum and from Swiss mice (P14 to P19) after lentivirus injection at P4 in the inferior olive. Briefly: mice were anesthetized by exposure to isoflurane 4% and sacrificed by decapitation. Cerebellum was dissected in ice cold oxygenated Bicarbonate Buffered Solution (BBS) containing (in mM): NaCl 120, KCl 3, $NaHCO_3$ 26, NaH_2PO_4 1.25, $CaCl_2$ 2 mM, $MgCl_2$ 1 and glucose 35. 280 µm sagittal slices were cut with a vibratome in the NMDG-based cutting buffer (in mM): NMDG 93, KCl 2.5, NaH_2PO_4 1.2, $NaHCO_3$ 30, HEPES 20, glucose 25, sodium ascorbate 5, thiourea 2, sodium pyruvate 3, $MgSO_4$ 10 and $CaCl_2$ 0.5 (pH 7.3). Immediately after cutting, slices were allowed to briefly recovery at 34°C in the oxygenated sucrose-based buffer (in mM): sucrose 230, KCl 2.5, $NaHCO_3$ 26, NaH_2PO_4 1.25, glucose 25, $CaCl_2$ 0.8 and $MgCl_2$ 8. D-APV and minocycline at a final concentration of 50 µM and 500 nM respectively were added to the sucrose-based and cutting buffers. Slices were allowed to fully recover in 95% O_2/5% CO_2 bubbled BBS at 34°C for at least 30 minutes before starting experiments.

Patch clamp borosilicate pipettes with 3-5 MΩ resistance were filled with the internal solution containing (in mM): $CsMeSO_3$ 135, NaCl 6, $MgCl_2$ 1, HEPES 10, MgATP 4, Na_2GTP 0.4,

EGTA 1.5 and QX314Cl 5 (pH 7.3). Stimulation electrodes with 5 MΩ resistance were pulled from borosilicate pipettes and filled with HEPES Buffered Solution (HBS) containing (in mM): NaCl 120, KCl 3, HEPES 10, NaH_2PO_4 1.25, $CaCl_2$ 2, $MgCl_2$ 1 and glucose 10 (pH7.3). The IsoStim A320 (WPI Inc, USA) stimulator was used to elicit CF and PF mediated responses in PC. Patch clamp experiments were conducted in voltage clamp mode using a MultiClamp 700B amplifier (Molecular Devices Inc, USA). Currents were low-pass filtered at 2 kHz and digitized at 20 kHz. Recordings were performed at room temperature on slices continuously perfused with 95% O_2/5% CO_2 bubbled BBS and in presence of picrotoxin 100 µM. CF and PF currents were monitored at a holding potential of respectively -10 mV and -60 mV.

During CF recordings the stimulation electrode was placed in the granule cells layer below the clamped cell; CF-mediated responses were identified by the typical all or nothing response and strong depression displayed by the second response elicited during paired pulse stimulations (20 Hz).

PF stimulation was achieved by placing the stimulation electrode in the molecular layer at the minimum distance required to avoid direct stimulation of the dendritic tree of the recorded PC. The input/output curve was obtained by incrementally increasing the stimulation strength. Peak EPSC values for PF were obtained following averaging of five consecutive traces and were normalized to the EPSC recorded at the lowest stimulus intensity in order to determine the fold increase in PF responses. Data analyses were performed with the scientific data analysis software Igor Pro (WaveMetrics, USA).

-Supplemental References

Avci, H.X., Lebrun, C., Wehrle, R., Doulazmi, M., Chatonnet, F., Morel, M.-P., Ema, M., Vodjdani, G., Sotelo, C., Flamant, F., et al. (2012). Thyroid hormone triggers the developmental loss of axonal regenerative capacity via thyroid hormone receptor alpha1 and kruppel-like factor 9 in Purkinje cells. Proc. Natl. Acad. Sci. U.S.A. *109*, 14206–14211.

Bally-Cuif, L., Alvarado-Mallart, R.M., Darnell, D.K., and Wassef, M. (1992). Relationship between Wnt-1 and En-2 expression domains during early development of normal and ectopic met-mesencephalon. Development *115*, 999–1009.

Fath T1, Ke YD, Gunning P, Götz J, Ittner LM. (2009). Primary support cultures of hippocampal and substantia nigra neurons. Nat Protoc. *4*, 78-85.

Tabata, T., Sawada, S., Araki, K., Bono, Y., Furuya, S., and Kano, M. (2000). A reliable method for culture of dissociated mouse cerebellar cells enriched for Purkinje neurons. J. Neurosci. Methods *104*, 45–53.